INFORMATION TO USERS

This manuscript has been reproduced from the microfilm master. UMI films the text directly from the original or copy submitted. Thus, some thesis and dissertation copies are in typewriter face, while others may be from any type of computer printer.

The quality of this reproduction is dependent upon the quality of the copy submitted. Broken or indistinct print, colored or poor quality illustrations and photographs, print bleedthrough, substandard margins, and improper alignment can adversely affect reproduction.

In the unlikely event that the author did not send UMI a complete manuscript and there are missing pages, these will be noted. Also, if unauthorized copyright material had to be removed, a note will indicate the deletion.

Oversize materials (e.g., maps, drawings, charts) are reproduced by sectioning the original, beginning at the upper left-hand corner and continuing from left to right in equal sections with small overlaps.

Photographs included in the original manuscript have been reproduced xerographically in this copy. Higher quality 6" x 9" black and white photographic prints are available for any photographs or illustrations appearing in this copy for an additional charge. Contact UMI directly to order.

Bell & Howell Information and Learning
300 North Zeeb Road, Ann Arbor, MI 48106-1346 USA
800-521-0600

UMI®

COMPUTATIONAL CHEMISTRY: MODELING OF POLYMER DEGRADATION BY ATOMIC OXYGEN IN LOW EARTH ORBIT

by

ASTA GINDULYTE

A dissertation submitted to the Graduate Faculty in Chemistry in partial fulfillment of the requirements for the degree of Doctor of Philosophy, The City University of New York

2000

This manuscript has been read and accepted for the Graduate Faculty in Chemistry in satisfaction of the dissertation requirement for the Degree of Doctor of Philosophy.

9/14/00
Date

Chair of Examining Committee

9/14/00
Date

Executive Officer

William E. L. Grossman

John R. Lombardi

Supervisory Committee

THE CITY UNIVERSITY OF NEW YORK

Acknowledgements

I express gratitude to my adviser prof. Lou Massa for all the support and advise during my graduate school years.

Many thanks go to Bruce A. Banks and Sharon K. Rutledge of NASA Glenn Research Center for their wonderful collaboration on the project.

I acknowledge the Maui High Performance Computational Center (MHPCC) for the allocation of computational time.

I am grateful to the members of the dissertation committee, profs. William E. L. Grossman and John R. Lombardi for all the suggestions during the committee meetings and careful reading of the manuscript.

I thank prof. Klaus Grohman for being a great graduate adviser.

CONTENTS

List of Tables

List of Figures

CHAPTER 1. Introduction

"Degradation of polymers by chemical reactions is a typical constitutive property. No methods for numerical estimations exist in this field. Only qualitative prediction is possible."

from *Properties of Polymers*, Elsevier, 1990

by D. W. van Krevelen and N. V. Arnhem

The space shuttle, the International Space Station (ISS), and many other satellites travel around the Earth through the space region called low Earth orbit (LEO), the altitudes of 180 to 650 kilometers above the Earth's surface. The largest component of the atmosphere at these altitudes is atomic oxygen (AO), which is created when oxygen molecules are split by short wavelength solar ultraviolet radiation in an environment where the mean free path is sufficiently large that the probability of recombination is negligible. The typical O-atom number density at space shuttle altitudes is on the order of 10^8 cm^{-3}. A LEO orbiting body typically travelling at 7.2 km/s relative to this density experiences a flux of 10^{14} O-atoms/cm^2s. Oxygen atoms hit the spacecraft surface with mean impact energies of ~4.5 eV (~100 kcal/mol).[1] Exposure to harsh LEO environment leads to significant changes in the condition of many spacecraft surface materials. Organic polymers that are used in LEO spacecraft to reduce weight in structures, insulation, and other components are particularly affected by LEO. These materials lose weight, and depending on thickness can be eroded away completely.[1-20]

The detrimental effects of LEO environment on spacecraft surface materials were first observed after early space shuttle missions.[2,10] Flight experiments were conducted during space shuttle flights STS-5,[11-14] STS-8,[15] STS-17,[15] STS-32,[16] STS-41,[16] and STS-44.[17] Long Duration Exposure Facility (LDEF)[18-19] and Limited Duration Candidate Exposure (LDCE) material exposure experiments[20] were conducted to develop fundamental understanding of the deleterious effects of the exposure of a variety of materials to the LEO environment. These experiments have demonstrated that although the ambient density of AO is quite low at altitudes where LEO spacecraft typically operate, the orbital speed of the spacecraft results in high incident fluxes and collisional energies large enough to interact with and degrade many material surfaces. Results of these experiments have also shown that prolonged exposure of sensitive spacecraft materials to the LEO environment will result in degraded system performance, which can significantly affect mission performance and may even result in premature mission failure.

Knowledge of the long-term durability of materials exposed to AO in the LEO environment is crucial to numerous space missions and experiments. Accurate quantification of AO effect on performance of spacecraft materials can significantly aid designers in selecting suitable materials and designing reliable spacecraft systems for the desired mission life at LEO altitudes. The need to understand and negate the adverse effects of AO erosion on spacecraft materials is of significant importance. Development of new materials and protective coatings which are stable in the LEO environment is an appealing approach to solving the AO degradation problem.[6]

In addition to space shuttle flights, the effects of AO interaction with various materials have been studied at ground-based laboratory facilities.[1,21-26] However, due to difficulties in simulating the LEO environment, the ground-based experiments generally fail to reproduce the AO erosion rates observed in LEO. The erosion yield of materials may be influenced by factors such as AO flux, AO fluence, synergistic solar radiation, AO impact energy, AO impact angle, material temperature, etc. Phenomenological models have been developed to explain the observed trends in materials degradation under a particular set of test conditions.[27] However, in spite of the research that has been done, to date there is no clear understanding of mechanisms for materials interaction with AO. Therefore, the ability to predict how a certain material would behave in LEO environment is very limited.

Given the importance of the problem of AO degradation of polymeric spacecraft materials in LEO, it would be appropriate to study this problem in a very fundamental way. The contribution of the present work is to suggest how the techniques of computational chemistry are to be used to begin a theoretical understanding of the problem. We are suggesting here for the first time that detailed quantum mechanical calculations may be used to study the interactions between AO and model molecules of materials that make up the layers of a spacecraft surface. Our approach to the problem is therefore microscopic or molecular. The great value of this approach is the possibility of examining all possible reactions between given reactants one at a time. Such a study can show which interactions lead to destructive chemical reactions. Moreover, quantum mechanics might also lead to an understanding of the relative rates at which such reactions occur. The ability to use

quantum mechanics to predict materials degradation by AO reaction mechanisms and relative reaction rates would be a capability of a great value to the space program.

We point out that the calculations of quantum mechanical energy surfaces, and their use in prediction of reaction mechanisms and rates is a well-practiced technology. It simply has never been applied to the complex problem of polymer degradation in LEO. In this thesis we show how this can be done. The general methodology is the following. Structures and energies of given reactants and desired products are computed. The energy difference between the products and the reactants is the enthalpy of the reaction (ΔH). Subsequently, the maximum of the potential energy surface (PES) connecting the reactants and products is located. This maximum or saddle point corresponds to the transition state structure of the chemical reaction. The energy difference between the transition state and the reactants is the activation energy of the reaction (E_a). These calculated properties (ΔH, E_a) may be used to order the expected outcomes of chemical reactions. In particular, reaction rate constants can often be estimated from the Arrhenius equation:

$$k = Ae^{-Ea/RT}$$

where k is the reaction rate constant, A is a constant called the pre-exponential factor, R is the universal gas constant, and T is temperature.

Without claiming to have solved the polymer degradation in LEO by AO problem in its entirety, we do claim to have shown how quantum mechanics can be used in a long-range program to obtain a comprehensive solution ultimately. Moreover, we have used quantum mechanics to obtain certain specific important results that are described in subsequent chapters.

In Chapter 2, the computational methods used in this work are discussed. In Chapter 3, the degradation of aliphatic hydrocarbons by AO is studied. Chapter 4 deals with degradation of fluoropolymers by AO. In Chapter 5, the AO reactions with benzene are examined. Chapter 6 contains a study of AO degradation of polymers that have aromatic rings in their backbones. In chapter 7, an attempt is made to correlate the measured LEO erosion rates to the structure of materials. Finally, chapter 8 contains the concluding remarks.

At last, we mention that the remark made by D. W. van Krevelen and N. V. Arnhem (beginning of this chapter) no longer holds, since in this work we have developed a method for numerical estimation of polymer degradation by chemical reactions.

References

(1) Banks, B. A.; de Groh, K. K.; Rutledge, S.; DiFilippo, F. J. NASA TM-107209, **1996**.

(2) Leger, L. J. NASA TM-58246, **1982**.

(3) Leger, L. J.; Visentine, J. T. *Aerospace America* **1986**, *24*, 32.

(4) Hunton, D. E. "Shuttle Glow." *Sci. Am.* **1989**, *261*, 92.

(5) Murr, L. E.; Kinard, W. H. "Effects of Low Earth Orbit." *Amer. Sci.* **1993**, *81*, 152.

(6) Reddy, M. R. *J. Mat. Sci.* **1995**, *30*, 281.

(7) Banks, B. A. "The Use of Fluoropolymers in Space Applications" In *Modern Fluoropolymers*; John Wiley & Sons: New York, **1997** and references therein.

(8) Gregory, J. NASA CP-3257.

(9) Dooling, D.; Finckenor, M. M. NASA TP-209260, **1999**.

(10) Leger, L. J. AIAA Paper 83-0073, **1983**.

(11) Peters, P. N.; Linton, R. C.; Miller, E. R. *Geophys. Res. Lett.* **1983**, *10*, 569.

(12) Leger, L. J., Spiker, I. K.; Kuminecz, T. J.; Ballentine, T. J.; Visentine, J. T. AIAA Paper 83-2631, **1983**.

(13) Park, J. J.; Gull, T. R.; Herzing, H.; Toft, A. R. AIAA Paper 83-2634, **1983**.

(14) Slemp, W. S. AIAA Paper 83-2633, **1983**.

(15) Visentine, J. T. NASA TM-100459, **1988**.

(16) Tennyson, R. C.; Morision, W. D.; Klemberg, J. E.; Martinu, L.; Wertheimer, M. R.; Zimick, D. G. AIAA Paper 92-2152, **1992**.

(17) Dunnet, A.; Kirkendal, T. D. in *Proceedings of the European Space Power Conference*; ESA-SP **1991**, *320*, 701.

(18) Levine, A. S. NASA CP-3134, **1992**.

(19) Levine, A. S. NASA CP-3194, **1993**.

(20) Schwam, D. *Space* **1993**, *9*, 14.

(21) Srinivasan, V.; Banks, B. A., Eds. *Materials Degradation in Low Earth Orbit*, Warrendale, Pa.: The Minerals, Metals and Materials Society, **1990**.

(22) Minton, T. K.; Nelson, C. M.; Brinza, D. E.; Liang, R. H. JPL, *Publication 91-34*, **1991**.

(23) Banks, B. A.; Rutledge, S. K.; Paulsen, P. E.; Steuber, T. J. NASA TM-101971, **1989**.

(24) Rutledge, S. K.; Banks, B. A.; DiFilippo, F.; Brady, J. A.; Dever, T.; Hotes, D. NASA TM-100122, **1986**.

(25) Garton, D. J.; Minton, T. K.; Alagia, M.; Balucani, N.; Casavecchia, P.; Volpi, G. G. *Discuss. Faraday Soc.* **1997**, *108*, 387.

(26) Kleiman, J. I.; Gudimenko, Y. I.; Iskanderova, Z. A.; Tennyson, R. C.; Morison, W. D.; McIntyre, M. S.; Davidson, R. *Surface and Interface Analysis* **1995**, *23*, 335.

(27) Iskanderova, Z. A.; Kleiman, J. I.; Gudimenko, Y. I.; Tennyson, R. C. *J. Spacecraft Rockets,* **1995**, *32*, 878.

CHAPTER 2. Computational Details

"If you want to make predictions, and not merely reproduce known results, you need to be able to judge the quality of your results. This is by far the most difficult task in computational chemistry."

from *Introduction to Computational Chemistry*, John Wiley & Sons, 1999

by F. Jensen

When trying to solve a problem with the use of computational chemistry, one is always faced with the need to choose a theoretical method or methods to be used. In order to succeed, one should be able to choose a method that is valid for that particular problem, and be able to answer the basic question: how good is the number that has been calculated? This requires much more experience and insight than just running a computer program. Understanding of theory behind the method is needed as well as knowledge of the performance of the method for chemical systems similar to the one that is being studied. If there is no previous experience for such systems, one needs to establish a way of calibrating the results. While the choice of the most sophisticated theoretical methods will almost always result in the best accuracy, it is not always feasible and/or practical to proceed in such fashion. The most sophisticated theoretical methods are also the most expensive in terms of computational resources and time.

The systems studied in this work are complicated in the context of computational chemistry. Since atomic oxygen in its ground state is a triplet, we studied reactions that proceed on a triplet potential energy surface (PES). It is far

more difficult (in terms of both computational cost and level of theoretical method required) to obtain accurate energy values for open-shell species than for closed-shell species. Furthermore, since we were mostly concerned with calculations of activation barriers of reactions, we needed to obtain energy values for transition state structures associated with these reactions. Again, it is more difficult to predict accurate energy values for the transition states than for equilibrium structures.

Since the progress of the problem (i.e., understanding of materials degradation by AO) depends not only on the quality of the results obtained, but also on their quantity (the more reaction mechanisms are studied, the better), we made it one of our objectives to come up with a computationally cost efficient scheme that would produce reasonably good results. There exist very few theoretical studies involving systems similar to the ones studied in this work, and therefore the performance of various methods had to be investigated. We applied a number of theoretical methods, ranging from the most sophisticated to a lot less expensive, to test cases (such as ethane reaction with O(3P) resulting in carbon-carbon bond breaking in Chapter 3 and O(3P) attack on π-electron density of benzene in Chapter 5). Larger related systems were treated with less expensive methods only. However, we were able to estimate the quality of these results based on our experience with the test cases.

All quantum mechanical calculations presented in this work were carried out with GAUSSIAN98[1] and MULLIKEN[2] program packages on an IBM/SP2 supercomputer at Hunter College and IBM/P2SC supercomputers at the Maui High Performance Computer Center (MHPCC). The reader is referred to ref. 3 for definitions of technical symbols used in this (and subsequent) chapters.

Traditional Hartree-Fock (HF)[4-6] and second order Möller-Plesset energy correction (MP2)[7-9] *ab initio* methods were used. (When calculating the relative energies for the systems where radicals were involved, PMP2 (spin-projected MP2) rather than MP2 energies were used.) Several hybrid DFT methods were applied. The Becke three-parameter-hybrid (B3)[10] was used in conjunction with three correlation functionals, the Lee-Yang-Parr (LYP),[11] Perdew 86 (P86),[12,13] and Perdew-Wang 91.[14] The MB3LYP method (see notes in ref. 15) available within MULLIKEN program package was also employed.

In addition, methods based on approximate procedures for estimating the "infinite correlation, infinite basis" limit were used in important test cases in order to obtain more accurate energy values. These methods were Complete Basis Set (CBS-QB3)[16] approach and Gaussian theoretical models (G1, G2, and G2MP2).[17-20] Differently from the standard G1, G2, and G2MP2 procedure, we used zero-point energy (ZPE) values obtained with the use of MP2 method rather than HF. For anharmonicity corrections these values were scaled by 0.9427.[21]

For all the calculations Gaussian-type basis sets were employed (see Table 3.1, for example). The explanation and abbreviations of the basis sets can be found in ref. 3.

The geometries of all reactants, products, and transition states have been optimized at the levels of theory mentioned above. For all open-shell species an unrestricted wave function was implemented and examined for spin contamination, which was found to be inconsequential. No symmetry constraints were imposed for optimizations of the transition states. Vibrational frequencies have been calculated

using the same approximation to characterize the nature of stationary points and to determine zero-point energy (ZPE) corrections. (When we refer to any calculated energy values in the text, we have in mind the ZPE corrected results.) All the stationary points have been positively identified for either minimum energy with no imaginary frequencies or for transition states with one imaginary frequency. In the cases where it was not clear (from the analysis of vibrational modes) whether a transition structure is connecting the desired reactants and products, intrinsic reaction coordinate (IRC) analysis was carried out in order to confirm that.

References

(1) Frisch, M. J.; Trucks, G. W.; Schlegel, H. B.; Scuseria, G. E.; Robb, M. A.; Cheeseman, J. R.; Zakrzewski, V. G.; Montgomery, J. A., Jr.; Stratmann, R. E.; Burant, J. C.; Dapprich, S.; Millam, J. M.; Daniels, A. D.; Kudin, K. N.; Strain, M. C.; Farkas, O.; Tomasi, J.; Barone, V.; Cossi, M.; Cammi, R.; Mennucci, B.; Pomelli, C.; Adamo, C.; Clifford, S.; Ochterski, J.; Petersson, G. A.; Ayala, P. Y.; Cui, Q.; Morokuma, K.; Malick, D. K.; Rabuck, A. D.; Raghavachari, K.; Foresman, J. B.; Cioslowski, J.; Ortiz, J. V.; Stefanov, B. B.; Liu, G.; Liashenko, A.; Piskorz, P.; Komaromi, I.; Gomperts, R.; Martin, R. L.; Fox, D. J.; Keith, T.; Al-Laham, M. A.; Peng, C. Y.; Nanayakkara, A.; Gonzalez, C.; Challacombe, M.; Gill, P. M. W.; Johnson, B.; Chen, W.; Wong, M. W.; Andres, J. L.; Gonzalez, C.; Head-Gordon, M.; Replogle, E. S.; Pople, J. A. *Gaussian 98,* Revision A.6; Gaussian, Inc.: Pittsburgh PA, **1998**.

(2) MULLIKEN is IBM proprietary software.

(3) Foresman, J. B.; Frisch, A. *Exploring Chemistry with Electronic Structure Methods*, 2nd ed.; Gaussian, Inc.: Pittsburgh, **1996**.

(4) Roothan, C. C. J.; *Rev. Mod. Phys.* **1951**, *23*, 69.

(5) Pople, J. A.; Nesbet, R. K. *J. Chem. Phys.* **1959**, *22*, 571.

(6) McWeeny, R.; Dierksen, G. *J. Chem. Phys.* **1968**, *49*, 4852.

(7) Möller, C.; Plesset, M. S. *Phys. Rev.* **1934**, *46*, 618.

(8) Saebo, S.; Almlof, J. *Chem. Phys. Lett.* **1989**, *154*, 83.

(9) Pople, J. A.; Binkley, J. S.; Seeger, R. *Int. J. Quant.Chem. Symp.* **1976**, *10*, 1.

(10) Becke, A. D. *J. Chem. Phys.* **1993**, *98*, 5648.

(11) Lee, C.; Yang, W.; Parr, R. G. *Phys. Rev. B* **1988**, *37*, 785.

(12) Perdew, J. P. *Phys. Rev. B* **1986**, *33*, 8822.

(13) Perdew, J. P. *Phys. Rev. B* **1987**, *34*, 7046.

(14) Perdew, J. P.; Wang, Y. *Phys. Rev. B* **1992**, *45*, 13244.

(15) P. J. Stephens, F. J. Devlin, C. F. Chabalowski,M. J. Frisch, *J. Phys. Chem.* **1994**, *98*, 11623. MB3LYP is very similar to B3LYP defined in this paper, except it uses the local correlation functional of Perdew and Wang (J. P. Perdew, Y. Wang, *Phys Rev. B* **1992**, *45*, 1324) instead of the Vosko, Wilk and Nusair functional.

(16) Montgomery, Jr., J. A.; Frisch, M. J.; Ochterski, J. W.; Petersson, G. A. *J. Chem. Phys.* **1999**, *110*, 2822.

(17) Pople, J. A.; Head-Gordon, M.; Fox, D. J.; Raghavachari, K.; Curtiss, L. A. *J. Chem. Phys.* **1989**, *90*, 5622.

(18) Curtiss, L. A.; Jones, C.; Trucks, G. W.; Raghavachari, K.; Pople, J. A. *J. Chem. Phys.* **1990**, *93*, 2537.

(19) Curtiss, L. A.; Raghavachari, K.; Trucks, G. W.; Pople, J. A. *J. Chem. Phys.* **1991**, *94*, 7221.

(20) Curtiss, L. A.; Raghavachari, K.; Pople, J. A. *J. Chem. Phys.* **1993**, *98*, 1293.

(21) Scott A. P.; Radom L. *J. Phys. Chem.* **1996**, *100*, 16502.

CHAPTER 3. AO Reactions with Aliphatic Hydrocarbons

While a material consisting entirely of long aliphatic hydrocarbon chains, polyethylene, is not extensively used as spacecraft surface material, there are reasons for understanding its erosion by AO mechanism. First, it has a simple chemical structure, and therefore it would seem that the degradation mechanisms would have to be among the simplest ones to study. Second, there are quite a few materials that are used or are being considered for use in spacecraft surface applications that contain fragments of $(CH_2)_n$ (n=1 or more) type in their polymer repeat units.

LEO observed erosion rates for polyethylene are among the highest for all organic polymers (~3.7×10^{-24} cm^3/O-atom).[1] Tests conducted at ground-based facilities showed that a low energy AO environment produces erosion rates orders of magnitude lower than those observed in space flights, while the erosion rates measured in fast AO beams are close to those observed in space.[2-4] The volatile products produced by AO reactions with the polymer surface are mainly OH radicals, H_2O, CO, and CO_2, but a small fraction of hydrocarbon fragments may also be present.[5,6]

Hydrogen abstraction reactions are well known between hydrocarbons and atomic oxygen in its ground state, O(3P). Moreover, it is usually assumed that hydrogen abstraction is the only type of reaction that would take place between saturated hydrocarbons and O(3P). However, given the unusual LEO conditions, e. g. oxygen atoms hitting the surface of polyethylene with impact energies ~100 kcal/mol, a possibility exists that O(3P) attacks on the carbon-carbon bonds, resulting in the breaking of polymer chains, could occur. In this work we use *ab initio* techniques to

investigate the reaction of O(3P) attack on carbon-carbon bonds of ethane and several higher alkanes, which we consider to be models, however simple, of polyethylene.

Computational Results

Reaction of ethane with O(3P): O(3P) + CH_3–CH_3 → •O–CH_3 + •CH_3.

The above reaction is a methyl abstraction from ethane by O(3P). The key geometric parameters computed by *ab initio* and DFT methods of the transition state structures for the ethane reaction with O(3P) are presented in Table 3.1. The classical and vibrational adiabatic (zero-point corrected) reaction barriers obtained by various DFT and *ab initio* methods are presented in Table 3.2.

There is no experimental evidence that suggests any information about the structure of the transition state. The appearance of this structure is very similar for all the theoretical methods used. The oxygen atom is almost aligned with the two carbon atoms. C1 and three hydrogen atoms attached to it lie in a plane, while C2 with its three hydrogen atoms form a pyramidal shape. A major disagreement among different methods is observed for the partially formed (O–C1) and partially broken (C1–C2) bonds of the transition state structure. HF calculated values for the above mentioned distances are very long as compared to MP2 and DFT methods. In addition, HF values obtained using a smaller basis set (3-21G) are in slightly better agreement with MP2 and DFT than those obtained using a larger basis set (6-31G(d,p)). Five different basis sets (double-zeta and triple-zeta with different numbers of polarization and diffusion functions) were used in conjunction with B3LYP method in order to explore the basis set effects. The geometrical parameters

for the transition state structure obtained with the use of these basis sets are all very close, with the exception of the 6-31G(d,p) basis set which calculates an O-C1 bond distance to be 1.775 Å as compared to 1.782-1.789 Å as obtained with the use of other basis sets. MB3LYP method gives almost identical structural parameters as the B3LYP method. B3P86 and B3PW91 both calculate slightly shorter distances than B3LYP and MB3LYP. MP2 method calculates yet shorter distances than all the DFT methods.

TABLE 3.1: Structural parameters (ångstroms and degrees) for the transition state of $C_2H_6 + O(3P) \rightarrow \bullet CH_3 + \bullet OCH_3$ reaction.

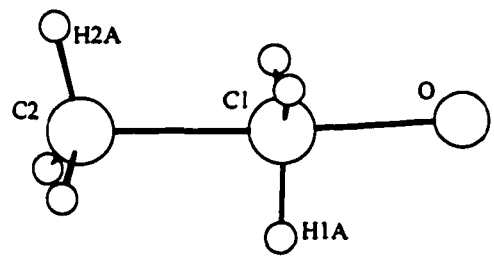

Theory	$r_{O\text{-}C1}$	$r_{C1\text{-}C2}$	$a_{O\text{-}C1\text{-}C2}$	$a_{O\text{-}C1\text{-}H1A}$	$a_{C1\text{-}C2\text{-}H2A}$
HF/3-21G	2.005	2.372	178.7	92.4	99.6
HF/6-31G(d,p)	2.157	2.488	178.9	91.2	99.1
MP2(Full)/6-31G(d)	1.723	1.920	176.6	94.2	106.0
MP2(FC)/6-31G(d,p)	1.721	1.920	176.3	94.4	105.9
MP2(FC)/6-31+G(d,p)	1.723	1.920	176.3	94.0	105.6
B3LYP/6-31G(d,p)	1.775	2.002	176.5	94.4	105.0
B3LYP/6-31+G (d,p)	1.789	2.008	176.8	93.8	104.4
B3LYP/6-311G(2d,2p)	1.782	2.005	177.1	93.7	104.4
B3LYP/6-311+G(2d,2p)	1.789	2.003	177.1	93.6	104.2
B3LYP/6-311++G(2d,2p)	1.789	2.003	177.1	93.6	104.2
B3P86/6-31+G(d,p)	1.753	1.968	176.5	94.2	105.0
B3P86/6-311+G(2d,2p)	1.754	1.963	176.7	94.0	104.7
B3PW91/6-31+G(d,p)	1.760	1.978	176.6	94.2	104.8
B3PW91/6-311+G(2d,2p)	1.759	1.972	176.8	94.0	104.6
MB3LYP/6-31+G(d,p)	1.789	2.008	176.9	93.8	104.5

There is no experimental measurement for activation energy of methyl abstraction from ethane by O(3P). It has been shown by Jursic[7] that a G1, G2, or G2MP2 computational approach calculates activation barriers for hydrogen abstraction from methane by O(3P) that are identical to the experimental value. This reaction is similar to the methyl abstraction from ethane in the sense that both reactions take place on a triplet potential energy surface, the reactants are a stable molecule and an oxygen atom in its ground state, and the products are two radicals. Therefore, we believe it is reasonable to assume that the G2 theory should perform well in this case too. Our calculated G2 activation barrier for the methyl abstraction from ethane by O(3P) is 44.5 kcal/mol. The activation energy for this reaction with the use of another method that is supposed to produce very accurate energy values, CBS-QB3, is 41.1 kcal/mol. The two results are within the error limits of the theoretical methods which are ~3 kcal/mol. The HF/3-21G value is 57.5 kcal/mol, and HF/6-31G(d,p) calculates it to be 60.9 kcal/mol. While both of these values are large overestimates over the G2 result, it seems that the use of the smaller basis set produces a slightly better result (at a lower computational cost too). The MP2 method in conjunction with moderate size basis sets produces the energy barrier ~4-7 kcal/mol higher than the G2 value. The DFT methods all calculate very similar values for the barrier, which is underestimated by ~6-9 kcal/mol as compared to the G2 result.

TABLE 3.2: Total energies (a. u.) and activation barriers (kcal/mol) for C_2H_6 + O(3P) → $\bullet CH_3$ + $\bullet OCH_3$ reaction.

Theory	E_{TS}	E_{C2H6}	E_O	E_a
HF/3-21G	-153.08712	-78.79395	-74.39366	63.1
HF/3-21G (0 K)	-153.01595	-78.71389	-74.39366	**57.5**
HF/6-31G(d,p)	-153.91529	-79.23823	-74.78393	67.1
HF/6-31G(d,p) (0 K)	-153.84591	-79.15902	-74.78393	**60.9**
MP2(Full)/6-31G(d)	-154.30254	-79.50397	-74.88329	53.2
MP2(Full)/6-31G(d) (0 K)	-154.22819	-79.42677	-74.88329	**51.4**
MP2(FC)/6-31G(d,p)	-154.33962	-79.54340	-74.88131	53.4
MP2(FC)/6-31G(d,p) (0 K)	-154.26508	-79.46594	-74.88131	**51.6**
MP2(FC)/6-31+G(d,p)	-154.35242	-79.54579	-74.88687	50.4
MP2(FC)/6-31+G(d,p) (0 K)	-154.27822	-79.46880	-74.88687	**48.6**
G1 (0 K)	-154.53544	-79.62498	-74.98205	**44.9**
G2 (0 K)	-154.54050	-79.62932	-74.98203	**44.5**
G2MP2 (0 K)	-154.53496	-79.62737	-74.97868	**44.6**
CBS-QB3 (0 K)	-154.55277	-79.63058	-74.98761	**41.1**
B3LYP/6-31G(d,p)	-154.83508	-79.83874	-75.06062	40.3
B3LYP/6-31G(d,p) (0 K)	-154.76302	-79.76381	-75.06062	**38.5**
B3LYP/6-31+G(d,p)	-154.84847	-79.84164	-75.06761	38.1
B3LYP/6-31+G(d,p) (0 K)	-154.77689	-79.76704	-75.06761	**36.2**
B3LYP/6-311G(2d,2p)	-154.88399	-79.86073	-75.08557	39.1
B3LYP/6-311G(2d,2p) (0 K)	-154.81216	-79.78617	-75.08557	**37.4**
B3LYP/6-311+G(2d,2p)	-154.89100	-79.86097	-75.09006	37.7
B3LYP/6-311+G(2d,2p) (0 K)	-154.81958	-79.78646	-75.09006	**35.7**
B3LYP/6-311++G(2d,2p)	-154.89106	-79.86098	-75.09006	37.6
B3LYP/6-311++G(2d,2p) (0 K)	-154.81955	-79.78647	-75.09006	**35.8**
B3P86/6-31+G(d,p)	-155.30779	-80.16827	-75.19989	37.9
B3P86/6-31+G(d,p) (0 K)	-155.23554	-80.09339	-75.19989	**36.2**
B3P86/6-311+G(2d,2p)	-155.34928	-80.18673	-75.22182	37.2
B3P86/6-311+G(2d,2p) (0 K)	-155.27773	-80.11204	-75.22182	**35.2**
B3PW91/6-31+G(d,p)	-154.78434	-79.81147	-75.03695	40.2
B3PW91/6-31+G(d,p) (0 K)	-154.71206	-79.73667	-75.03695	**38.6**
B3PW91/6-311+G(2d,2p)	-154.82514	-79.82941	-75.05869	39.5
B3PW91/6-311+G(2d,2p) (0 K)	-154.75343	-79.75483	-75.05869	**37.7**
MB3LYP/6-31+G(d,p)	-154.75243	-79.77573	-75.03772	38.3
MB3LYP/6-31+G(d,p) (0 K)	-154.68065	-79.70123	-75.03772	**36.6**

Reactions of higher alkanes (n=1,2,3) with O(3P): O(3P) + CH_2–$(C_nH_{2n+1})_2$ → $\bullet O$–CH_2–(C_nH_{2n+1})+ $\bullet C_nH_{2n+1}$. The key geometric parameters

computed by HF and DFT methods of the transition state structures for the reactions of propane, pentane and heptane with O(3P) (where the O(3P) attacks the central carbon atom) are presented in Table 3.3. The classical and vibrational adiabatic (zero-point corrected) reaction barriers obtained by HF and DFT methods are presented in Table 3.4.

TABLE 3.3: Structural parameters (ångstroms and degrees) for the transition state of $O(3P) + CH_2{-}(C_nH_{2n+1})_2 \rightarrow \bullet O{-}CH_2{-}(C_nH_{2n+1}) + \bullet C_nH_{2n+1}$, where n=1,2,3, reaction.

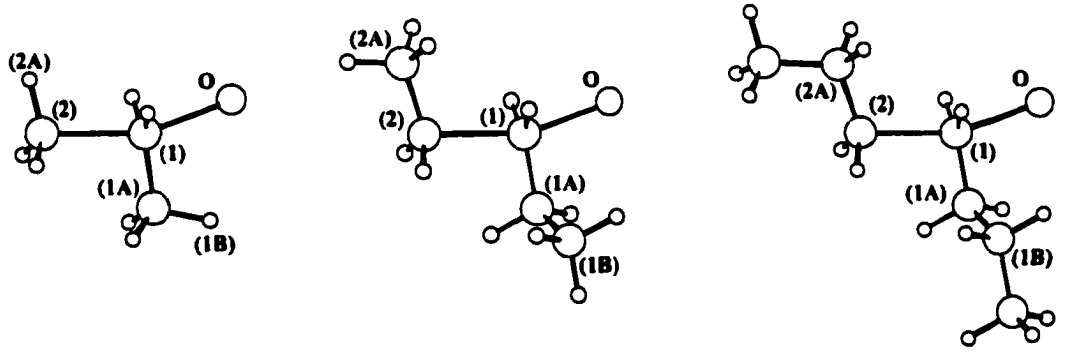

n	Theory	$r_{O\text{-}1}$	$r_{1\text{-}2}$	$a_{O\text{-}1\text{-}2}$	$a_{O\text{-}1\text{-}1A}$	$a_{1\text{-}2\text{-}2A}$	$d_{2\text{-}1\text{-}1A\text{-}1B}$	$d_{O\text{-}1\text{-}1A\text{-}1B}$
1	HF/3-21G	2.119	2.500	162.9	100.5	99.5	178.7	-1.4
2		2.135	2.434	163.3	96.2	105.8	-105.6	71.9
3		2.141	2.444	163.2	96.4	106.5	-106.1	71.6
1	MB3LYP/6-31+G (d,p)	1.814	2.034	159.1	102.5	104.7	-173.9	6.8
2		1.843	2.033	160.1	99.1	109.1	-100.7	77.5
3		1.841	2.033	160.1	99.2	109.8	-100.7	77.6

There are several differences in the structures of the transition states for the reactions of higher alkanes as compared to the ethane case. First, the partially formed (O–C1) and partially broken (C1–C2) bonds are longer. Second, the oxygen atom is no longer aligned with the two carbon atoms. The O–C1–C2 angle is ~160° as

opposed to almost 180° in the case of ethane. In addition, in the case of pentane and heptane there is a considerable rotation around the C1–C1A bond, which results in a dihedral angle, C2-C1-C1A-C1B, of —100° as opposed to 0° in the hydrocarbon chain. The cause of these differences is certainly the repulsion between the oxygen atom and the groups attached to the carbon atom that is being attacked by O(3P).

Despite the considerable differences in the geometrical parameters between the transition states of higher alkanes and that of ethane, the energy barriers for the reaction remain almost the same. HF/3-21G produces a barrier of 58.4, 57.9, and 58.0 kcal/mol for propane, pentane, and heptane, respectively, as opposed to 57.5 kcal/mol for ethane. MB3LYP/6-31+G(d,p) calculated values for the barrier are 38.5, 36.3, and 36.5 kcal/mol for propane, pentane, and heptane, respectively, as opposed to 36.6 kcal/mol for ethane.

TABLE 3.4: Total energies (a. u.) and activation barriers (kcal/mol) for O(3P) + CH_2–$(C_nH_{2n+1})_2$ → •O–CH_2–(C_nH_{2n+1})+ •C_nH_{2n+1}, where n=1,2,3, reaction.

n	Theory	E_{TS}	$E_{CH2-(CnH2n+1)2}$	E_O	E_a
1	HF/3-21G	-191.90475	-117.61330	-74.39366	64.1
	HF/3-21G (0 K)	-191.80296	-117.50234	-74.39366	**58.4**
2	HF/3-21G	-269.54560	-195.25156	-74.39366	62.5
	HF/3-21G (0 K)	-269.38074	-195.07937	-74.39366	**57.9**
3	HF/3-21G	-347.18386	-272.88977	-74.39366	62.5
	HF/3-21G (0 K)	-346.95773	-272.65646	-74.39366	**58.0**
1	MB3LYP/6-31+G (d,p)	-194.03759	-119.06365	-75.03772	40.0
	MB3LYP/6-31+G (d,p) (0 K)	-193.93709	-118.96072	-75.03772	**38.5**
2	MB3LYP/6-31+G (d,p)	-272.61775	-197.63923	-75.03772	37.1
	MB3LYP/6-31+G (d,p) (0 K)	-272.45972	-197.47977	-75.03772	**36.3**
3	MB3LYP/6-31+G (d,p)	-351.19319	-276.21478	-75.03772	37.2
	MB3LYP/6-31+G (d,p) (0 K)	-350.97855	-275.99894	-75.03772	**36.5**

Discussion and Conclusions

In this work we investigated one of the possible reaction pathways leading to the erosion of hydrocarbons by O(3P), viz., the chain breaking of a hydrocarbon caused by a single O(3P) attack. We used HF, DFT, MP2, CBS-QB3 and G2 theoretical methods to compute the energy barrier for such a reaction in ethane. The variation in values for the energy barrier was quite appreciable among the different methods. We believe that the most reliable estimates are the results obtained by the use of the G2 and CBS-QB3 method, ~40-45 kcal/mol. We extended the investigation to the cases of propane, pentane and heptane, using HF and DFT methods only. The results, i. e., the reaction barriers for the reactions of the higher alkanes with O(3P), were very close to those of ethane, computed by the use of the same theoretical methods. This suggests that rather small molecules (in contrast to long polymer chains) can be used in modeling the reactions of O(3P) with materials without compromising the accuracy of the results. In addition, it seems that HF is likely to overestimate the value of the energy barrier for the reaction as compared to the G2 method, while DFT is likely to underestimate this value as compared to G2. Therefore, we believe that (for the sake of lower computational cost) these two methods can be used for the study of analogous reactions in similar systems in order to obtain an upper and a lower bound for the value of the energy barrier.

Experimental activation energies for the hydrogen abstraction reactions by O(3P) determined for various saturated hydrocarbons in the gas phase are 6.9, 4.5, 3.3 kcal/mol for the primary, secondary, and tertiary hydrogen atoms, respectively.[8] The experimental energy barrier for the hydrogen abstraction by O(3P) from methane is

9.0–11.4 kcal/mol.[9] Thus, it is clear that hydrogen abstraction (and resulting subsequent reactions) is the low energy pathway to hydrocarbon erosion by O(3P). However, oxygen atoms in LEO collide with spacecraft surfaces at impact energies of ~100 kcal/mol (the top of the Maxwellian distribution of speeds). We have shown here the collision energy available in LEO is more than enough to overcome the energy barrier (~45 kcal/mol) for hydrocarbon chain breaking, therefore, making an occurrence of such reactions in the LEO environment a definite possibility.

It is interesting to note, that while the ratio of H to C atoms in a linear hydrocarbon chain is 2:1, the ratio of hydrogen abstraction to chain breaking sites is 1:1 (see Figure 3.1). This is due to the fact that the same carbon atom can be attacked from two sides. Therefore, we speculate that from the geometrical point of view (in contrast to the energetical point of view) the two types of reactions might be equally probable.

Figure 3.1. Possible sites for O(3P) attack on a hydrocarbon fragment. Short arrows indicate the hydrogen abstraction sites, and broken arrows indicate the chain breaking reaction sites.

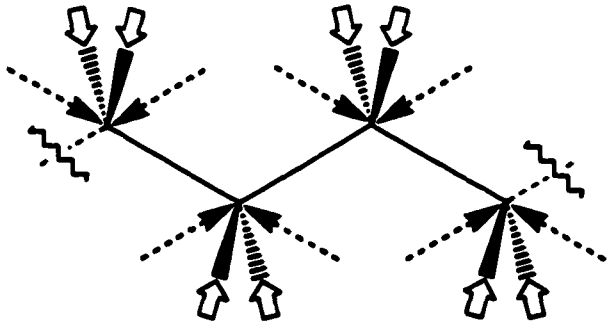

The occurrence of chain breaking reactions (in addition to hydrogen abstraction and all other related reactions) could greatly accelerate the erosion of hydrocarbons caused by O(3P). In Figure 3.2 we provide a scheme for the degradation of a hydrocarbon via chain breaking reactions with O(3P). First, the polymer chain is broken by a single O(3P) attack. Second, occurrence of another such reaction at an arbitrary site of the polymer chain, disrupts the chain again, creating a loose fragment. If that newly created fragment is small enough, it could probably leave the surface altogether. Therefore, it takes only one step to disrupt the polymer chain, and two steps to create a microscopic pit in it.

In Figure 3.3 we depict how the hydrocarbon chain could be disrupted via hydrogen abstraction, assuming one of the most efficient pathways. First, a hydrogen atom is abstracted by O(3P), creating an OH radical (which, of course, could contribute to the degradation too, although we do not consider that here) and a radical site on the hydrocarbon chain. Second, O(3P) abstracts a hydrogen atom belonging to a carbon atom nearest neighbor of the carbon atom from the first step. Here, either a double bond between the two carbon atoms, or two neighboring radical sites are created. Third, O(3P) can react with either the double bond or the two neighboring radical sites, thus, resulting in an epoxide. In order for the chain to be broken, the fourth oxygen atom has to attack one of the carbon atoms in the epoxide structure. Therefore, it takes at least four steps to break the hydrocarbon chain via this mechanism, while the same result could be accomplished in just one step via the chain breaking pathway.

Figure 3.2. Proposed aliphatic hydrocarbon erosion mechanism via chain breaking reactions with O(3P).

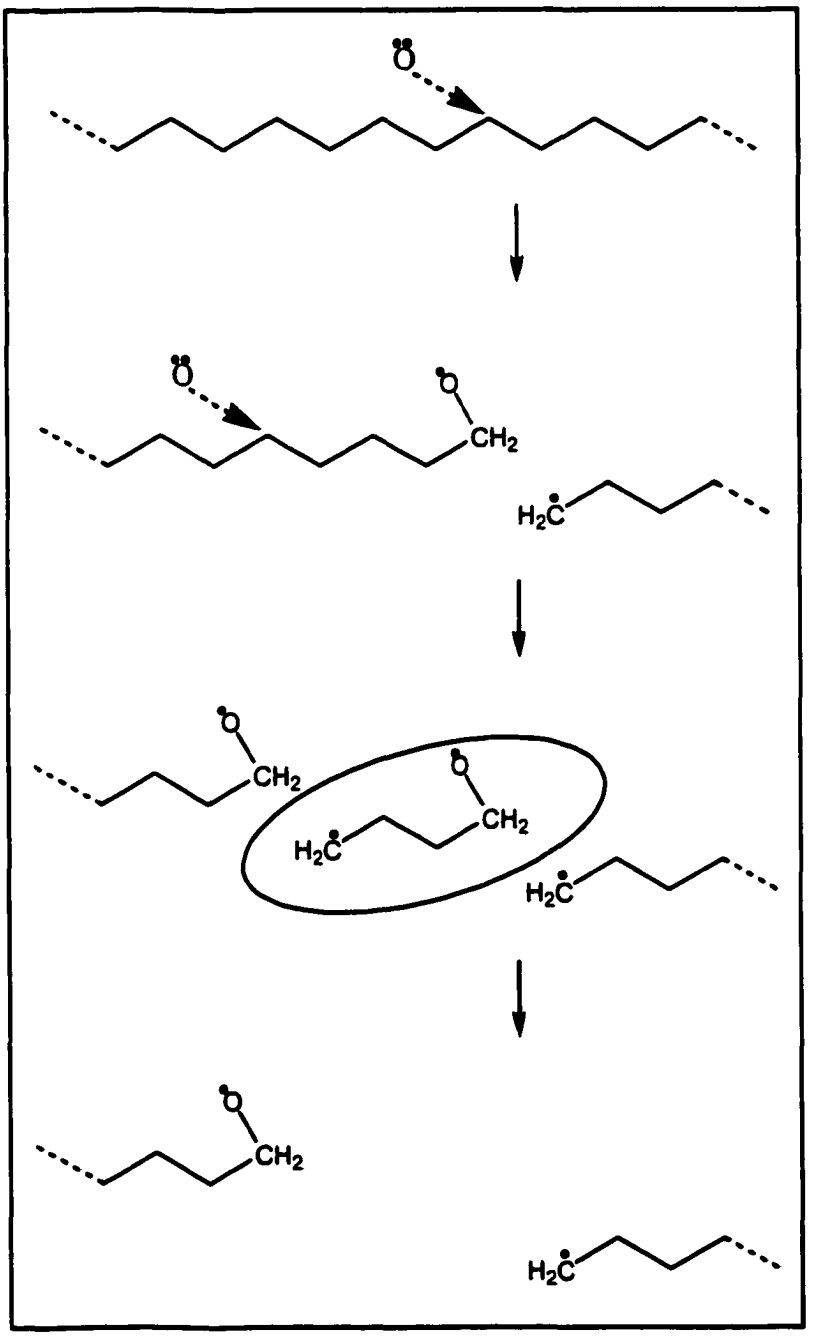

Figure 3.3. Proposed aliphatic hydrocarbon erosion mechanism via hydrogen abstraction reactions with O(3P).

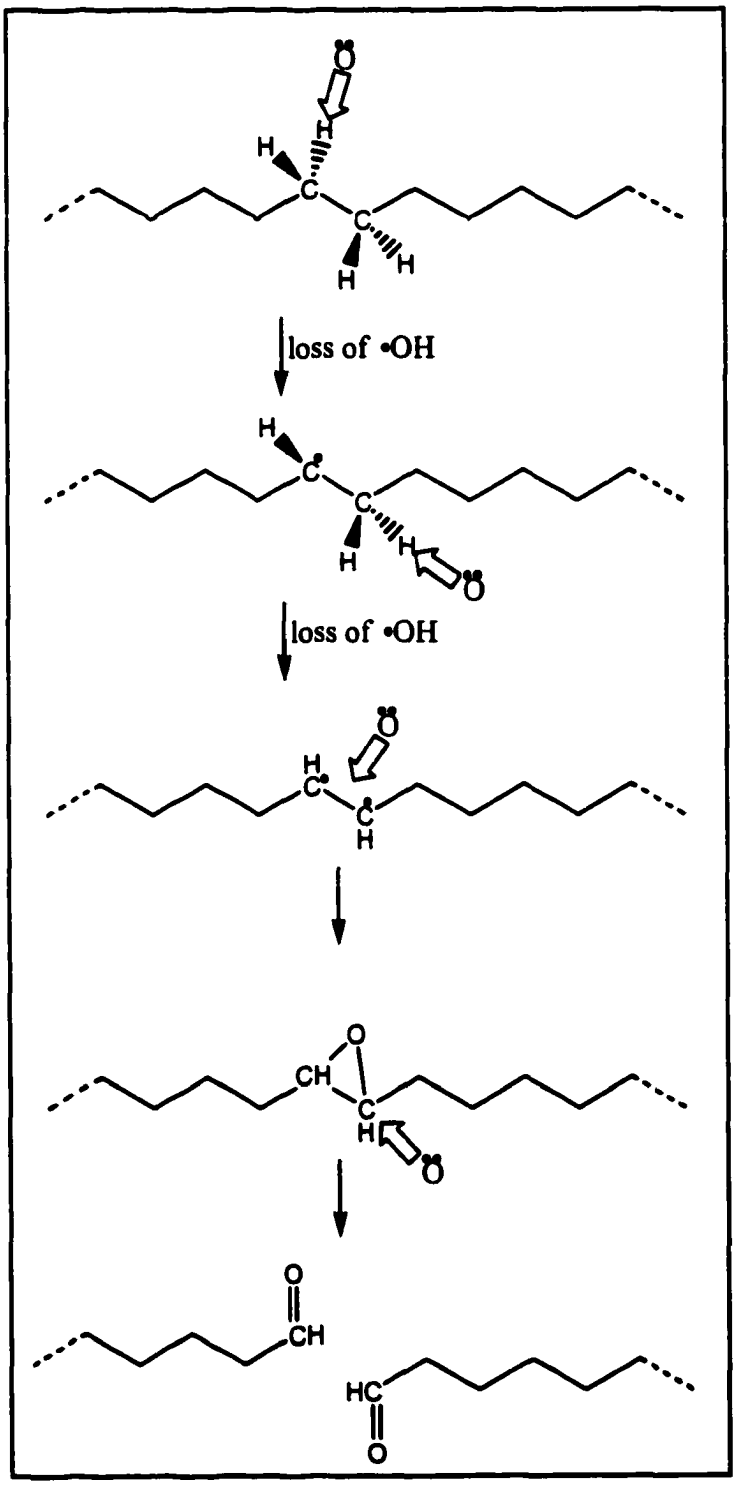

In summary, we have calculated the activation barrier for a chain breaking mechanism associated with O(3P) attack on a hydrocarbon chain. We have studied four small alkanes as models of polyethylene. The magnitude of the activation barrier is similar for all these cases, making it a probable magnitude for longer polyethylenes too. Importantly, we have established the calculated barriers (~40-45 kcal/mol) are substantially less than the O(3P) kinetic energy available in LEO. Thus, chain breaking studied here is certainly an important candidate mechanism for contributing to polyethylene degradation in LEO. Moreover, chain breaking appears to be entropically advantageous over hydrogen abstraction mechanisms. If chain breaking is in fact an important contributor to degradation, this may affect which strategies are employed to predict the erosion rates of materials in LEO at ground-based facilities.

Finally, we point out that in so far as the chain breaking mechanism might be important to degradation in space experiments, where O(3P) kinetic energy greatly exceeds our calculated E_a of ~40-45 kcal/mol, it follows that for those ground based plasma asher experiments with O(3P) kinetic energy (~1 kcal/mol, at energy distribution peak), which is much less than the activation energy, the same reaction would be much less probable. Note also, that the hydrogen abstraction reactions would also be a lot less probable in plasma ashers. This would explain the great reduction in reaction probability in ground based AO plasma asher experiments compared to AO in space. The relative contributions to the erosion rates of the two different mechanisms is not clear, but should be highly dependent on AO energy, and thus, experimental measurements of the polyethylene erosion rates dependence on AO incident energy in the range of 0.1-10 eV would help to understand this.

References

(1) Banks, B. A. "The Use of Fluoropolymers in Space Applications." In *Modern Fluoropolymers*; John Wiley & Sons: New York, **1997**.

(2) Koontz, S. L.; Albyn, K. A.; Leger, L. J. "Atomic Oxygen Testing with Thermal Atom Systems: A Critical Evaluation." *J. Spacecraft Rockets* **1991**, *28*, 315.

(3) Tennyson, R. C. "Atomic Oxygen Effects on Polymer-Based Materials." *Can. J. Phys.* **1991**, *69*, 1190.

(4) Chambers, A. R.; Harris, I. L.; Roberts, G. T. "Reactions of Spacecraft Materials with Fast Atomic Oxygen." *Materials Letters* **1996**, *26*, 121.

(5) Garton, D. J.; Minton, T. K.; Alagia, M.; Balucani, N.; Casavecchia, P.; Volpi, G. G. "Reactive Scattering of Ground-State and Electronically-Excited Oxygen Atoms on a Liquid Hydrocarbon Surface." *Discuss. Faraday Soc.* **1997**, *108*, 387.

(6) Cazaubon, B.; Paillous A.; Siffre, J. "Mass Spectrometric Analysis of Reaction Products of Fast Oxygen Atoms-Materials Interactions." *J. Spacecraft Rockets* **1998**, *35*, 797.

(7) Jursic, B. S. *J. Mol. Struct. (THEOCHEM)* **1998**, *427*, 137.

(8) Andresen, P.; Luntz, A. C. *J. Chem. Phys.* **1980**, *72*, 5842.

(9) Gonzalez, C.; MacDouall, J. J. M.; Schlegel, H. B. *J. Phys. Chem.* **1990**, *94*, 7467 and references therein.

CHAPTER 4. AO Reactions with Fluoropolymers

Spacecraft flying in LEO require thermal control blankets which provide protection from solar heating.[1] One of the materials used extensively for spacecraft thermal control is FEP (fluorinated ethylene propylene) Teflon®, which has its second (unexposed) surface metalized with silver or aluminum. The spacecraft thermal control is achieved by means of high reflection of incident solar energy (which has an intensity peak near 0.55 μm) and high thermal emittance of FEP Teflon® at spacecraft temperatures (which radiate near 10 μm). Other similar forms of thermal control surfaces or blankets consist of white Tedlar® (PVF (polyvinylidene fluoride)) and beta-cloth (PTFE (polytetrafluoroethylene) impregnated woven fiberglass). These two thermal control materials rely upon the low solar absorptance of their white color rather than second surface reflection from bright metals to reduce solar heating. Their emittance, similar to FEP Teflon®, is based on the emittance of the bulk white PVF or PTFE impregnated fiberglass.

FEP Teflon® is susceptible to erosion, cracking, and subsequent mechanical failure in LEO.[2] The textured surface produced by atomic oxygen causes light to reflect diffusely as opposed to specularly from a smooth surface.[1] Although the change from a specular surface to a diffuse surface has little if any effect on the total reflectance or absorptance of a metalized thermal control blanket, the recession of surface due to atomic oxygen attack does cause a reduction in thermal emittance.

One of the difficulties in determining whether FEP Teflon® will survive during a mission is the wide disparity of erosion rates observed for this material in space and in ground based facilities.[2] (The erosion rates observed in ground based

facilities generally greatly exceed those observed in space.) Each environment contains different concentrations of oxygen atoms and ions, and different levels of vacuum ultraviolet (VUV) radiation in addition to parameters such as the energy of arriving species and temperature. These variations make it difficult to determine what is causing the observed differences in erosion rates.

It has been proposed that high erosion rates of the FEP Teflon® observed in low energy AO ground-based laboratory facilities are due to significant VUV exposure (at higher levels than in space).[3] Moreover, samples exposed to low energy AO but not VUV showed a mass loss rate not significantly different from zero.[3] Indeed there is evidence that exposure to VUV produces chain scission radicals in FEP Teflon® (while the C-F bond scission products are not observed).[4,5] These radicals can react with atomic oxygen and volatile products may form. In addition, ground-simulation test results show that FEP Teflon®, exposed to VUV radiation only, suffered no thickness loss and possessed a hard embrittled surface layer (attributed to crosslinking) which was absent in the samples exposed to VUV and AO simultaneously.[3,6] Therefore, it was concluded that there is a strong synergistic effect between VUV and AO.

On the other hand, the conclusion drawn from another experimental study (also performed at low energy AO ground-based laboratory facilities) is that it does not appear to matter whether, in addition to AO, the samples are simultaneously exposed to VUV radiation, but the increase in the erosion rates is due to charged species (electrons and oxygen ions) present in the system.[2]

Tests have also been conducted at fast AO beam facilities with simultaneous exposure to VUV where incident AO energy was ~5 eV[7] and ~30 eV[8], and the erosion rates were higher than those observed in space by one and three orders of magnitude, respectively. At a facility[9] where it was possible to expose materials to a relatively fast (~2.2 eV) energy AO beam without VUV presence, the erosion rate was very low and close to that observed in some space flights (the erosion rates of FEP Teflon® measured in space experiments can also differ significantly[10]), but greatly increased when VUV was added.

Despite all the experimental work, to date there is no clear understanding of fluoropolymer erosion mechanisms in LEO, and the use of ground based simulation facilities for space materials qualification may lead to erroneous conclusions. An especially important question that is unanswered to date is how the fluoropolymer erosion rates depend on AO incident energy. Therefore, it is not known whether an exposure to oxygen atoms with incident energy of ~5 eV (LEO environment) without the presence of VUV can cause the erosion. If such a process is indeed possible, it may be an important contributor to the degradation rates observed in LEO in addition to possible AO/VUV synergistic effects. It is a possibility that the two phenomena may be competing, and the relative contributions of each would depend on the AO flux, AO incident energy, and the levels of VUV radiation present. In this work we seek to answer the question whether an exposure to oxygen atoms with incident energy of ~5 eV without the presence of VUV can cause the erosion.

PTFE (as well as fragments of the FEP Teflon® polymer chain) has a similar structure to that of polyethylene, differing only by substitution of fluorine atoms for

hydrogen atoms. The electronegativity of fluorine would seem to preclude an abstraction mechanism similar to that which occurs in the case of hydrogen. On the other hand, the results of the previous chapter suggest the possibility that chain breaking by O(3P) could be a contributing cause of degradation.

Computational Results

Chain breaking reactions of O(3P) with C_2F_6, C_3F_8, and C_5F_{12}, where in the case of C_3F_8 and C_5F_{12}, O(3P) attacks the central carbon atom, were studied in this work. The key geometric parameters computed by HF and DFT methods of the transition state structures for these reactions are presented in Table 4.1. The classical and vibrational adiabatic (zero-point corrected) reaction barriers obtained by HF and DFT methods are presented in Table 4.2. As is the case with the alkane analogs (studied in the previous chapter), there is no experimental evidence that would suggest any information about the structures of the transition states or the energy barriers associated with these reactions.

The appearance of the transition state structure for O(3P) reaction with C_2F_6, is similar to that of O(3P) reaction with C_2H_6. The oxygen atom is almost aligned with the two carbon atoms. C1 and three fluorine atoms attached to it lie in a plane, while C2 with its three fluorine atoms form a pyramidal shape. A major difference between the hydrogenated and fluorinated analogs is observed for the partially formed (O–C1) and partially broken (C1–C2) bonds of the transition state structure as calculated with the use of HF theoretical method. The O-C1 bond length is 2.914 Å and 2.005 Å for C_2F_6 and C_2H_6 cases, respectively. Similarly, the C1-C2 bond

length is 2.746 Å and 2.372 Å. The bond length values calculated with the use of MB3LYP DFT method are very similar and slightly smaller than those in the case of C_2H_6, i. e., 1.765 Å for O-C1 bond and 1.920 Å for C1-C2 bond.

TABLE 4.1: Structural parameters for the transition states of O(3P) reactions with C_2F_6, C_3F_8, and C_5F_{12}, where in the case of C_3F_8 and C_5F_{12} the oxygen atom attacks the center carbon atom.

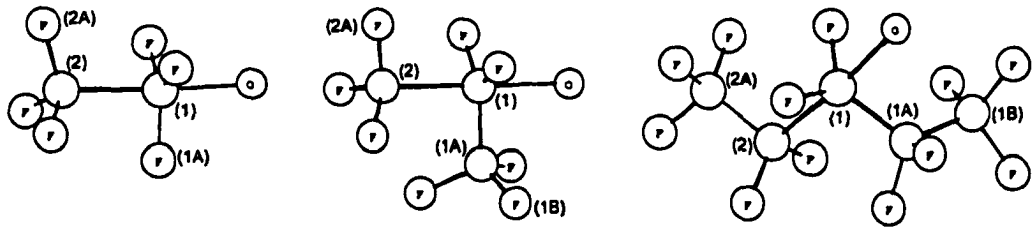

Model molecule	Theory	$r_{O\text{-}1}$	$r_{1\text{-}2}$	$a_{O\text{-}1\text{-}2}$	$a_{O\text{-}1\text{-}1A}$	$a_{1\text{-}2\text{-}2A}$	$d_{2\text{-}1\text{-}1A\text{-}1B}$	$d_{O\text{-}1\text{-}1A\text{-}1B}$
C_2F_6	HF/3-21G	2.914	2.746	174.2	81.9	102.7	—	—
C_3F_8		2.974	2.725	175.5	79.8	93.5	-122.3	61.1
C_5F_{12}		X	X	X	X	X	X	X
C_2F_6	MB3LYP/6-31+G(d,p)	1.765	1.920	176.7	92.5	107.8	—	—
C_3F_8		1.830	2.011	173.4	85.2	102.6	-103.3	71.0
C_5F_{12}		1.873	2.066	172.8	84.7	109.3	99.2	-74.6

The fluorinated case differs from the hydrogenated case in two ways. First, highly electronegative fluorine atoms withdraw some electron density from the carbon atom that is being attacked by oxygen and therefore, the oxygen atom would have to be slightly closer to the carbon atom in order for a bonding interaction to take place. Second, there is a repulsive interaction between the highly electronegative fluorine atoms and the oxygen atom. These two interactions have opposite effect on

the bond lengths. The latter effect seems to be strongly favored by the HF method which does not account for electron correlation. These results emphasize that electron correlation is especially important in complex systems such as transition states which involve bond breaking and forming. Since DFT methods do account for electron correlation the results obtained by the use of these methods are definitely more trustworthy.

The two effects described above offer a possible explanation for the high activation energy for the fluorinated case, i. e., 94.6 kcal/mol and 79.8 kcal/mol as obtained with the use of HF and DFT methods, respectively. Based on our previous experience with C_2H_6, we believe that these two numbers are high and low bounds for the activation energy of the reaction.

TABLE 4.2: Total energies (a. u.) and activation barriers (kcal/mol) for the transition states of O(3P) reactions with C_2F_6, C_3F_8, and C_5F_{12}, where in the case of C_3F_8 and C_5F_{12} the oxygen atom attacks the center carbon atom.

Model molecule	Theory	E_{TS}	E_{model}	E_O	E_a
C_2F_6	HF/3-21G	-742.98149	-668.74490	-74.39366	98.6
	HF/3-21G (0 K)	-742.95561	-668.71264	-74.39366	94.6
C_3F_8	HF/3-21G	-978.47485	-904.20508	-74.39366	77.7
	HF/3-21G (0 K)	-978.43497	-904.15945	-74.39366	74.1
C_5F_{12}	HF/3-21G				X
	HF/3-21G (0 K)				X
C_2F_6	MB3LYP/6-31+G (d,p)	-749.95470	-675.04639	-75.03772	81.2
	MB3LYP/6-31+G (d,p) (0 K)	-749.92822	-675.01763	-75.03772	79.8
C_3F_8	MB3LYP/6-31+G (d,p)	-987.67601	-912.74698	-75.03772	68.2
	MB3LYP/6-31+G (d,p) (0 K)	-987.63678	-912.70611	-75.03772	67.2
C_5F_{12}	MB3LYP/6-31+G (d,p)	-1463.07482	-1388.14563	-75.03772	68.1
	MB3LYP/6-31+G (d,p) (0 K)	-1463.01145	-1388.08061	-75.03772	67.1

The transition state structures for the reactions of O(3P) with C_3F_8 and C_5F_{12}, obtained with the use of MB3LYP DFT method, are similar to what we would expect based on our experience with the O(3P) reactions with alkanes. The bonds that are being broken and formed are slightly longer than in the C_2F_6 case, and the O-C1-C2 angle is slightly smaller due to the repulsion between the oxygen atom and the groups attached to the carbon atom that is being attacked by O(3P). We were unable, however, to obtain the result for the C_5F_{12} case with the use of HF method due to convergence problems which, we believe, arose because of the unrealistically long partially broken and formed bonds.

The activation energy values for the reactions of O(3P) with C_3F_8 and C_5F_{12}, obtained with the use of MB3LYP DFT method, are 67.2 kcal/mol and 67.1 kcal/mol, respectively. The activation energy value for the reaction of O(3P) with C_3F_8 obtained with the use of HF method, is 74.1 kcal/mol. The similarity of the two DFT results encourages us to estimate the activation energy value for longer fluoropolymer chains at ~70-80 kcal/mol.

Conclusions

We conclude that the chain breaking reactions of AO with fluoropolymer chains are possible under LEO conditions where the oxygen atoms possess translational energy on the order of ~100 kcal/mol. The relative importance of this contribution in comparison to that of AO/VUV synergy is not clear, but can be expected to be highly sensitive to the factors such as levels of VUV radiation, AO flux, and AO incident energy. It may be that the wide disparity of erosion rates

observed for fluoropolymers in space and in ground based facilities is the result of measurement the degradation occurring due to a different phenomenon. Therefore, there is a need of experimental measurements of fluoropolymers erosion rates exposed to fast neutral AO beams with AO energy distribution comparable to that of LEO environment without the simultaneous exposure to VUV. Higher energy beams might increase the erosion rates due to increased probability of chain breaking reactions, while the use of a lower energy beam would result in decreased probability of such reactions. (Indeed, the exposure of FEP Teflon to ~2.2 eV (~50 kcal/mol) energy AO beam without VUV presence, resulted in very low erosion rates.)

References

(1) Banks, B. A. "The Use of Fluoropolymers in Space Applications." In *Modern Fluoropolymers*; John Wiley & Sons: New York, **1997**.

(2) Rutledge, S. K.; Banks, B. A.; Kitral, M. "A Comparison of Space and Ground Based Facility Environmental Effects for FEP Teflon." NASA TM-207918/REV1, **1998**.

(3) Koontz, S. L.; Leger, L. J.; Albyn, K. A.; Cross, J. "Ultraviolet Radiation/Atomic Oxygen Synergism in Materials Reactivity." *J. Spacecraft and Rockets* **1990**, *27*, 346.

(4) Kim, S. S.; Liang, R. H. *Polym. Prepr.* **1990**, *31*, 389.

(5) Rasoul, F. A.; Hill, D. J. T.; George, G. A.; O'Donnell J. H. "A Study of a Simulated Low Earth Environment on the Degradation of FEP Polymer." *Polymers for Advanced Technologies* **1998**, *9*, 24.

(6) Rousslang, K.; Crutcher, Pippin, H. G. Proceedings of the First LDEF Post-retrieval Symposium, NASA CP-3134(2), 847, **1992**.

(7) Chambers, A. R.; Harris, I. L.; Roberts, G. T. "Reactions of Spacecraft Materials with Fast Atomic Oxygen." *Materials Letters* **1996**, *26*, 121.

(8) Vered, R.; Matlis, S.; Nahor, G.; Lempert, G. D.; Grossman, E.; Marom, G.; Lifshitz, Y. *Surface and Interface Analysis* **1994**, *22*, 532.

(9) Tennyson, R. C. "Atomic Oxygen Effects on Polymer-Based Materials." *Can. J. Phys.* **1991**, *69*, 1190.

(10) Reddy, M. R. "Review Effect of Low Earth Orbit Atomic Oxygen on Spacecraft Materials" *J. Mat. Sci.* **1995**, *30*, 281.

CHAPTER 5. AO Reactions with Benzene

Aromatic rings are present in the backbone of many polymers that are of interest to LEO spacecraft designers. Therefore, understanding of AO degradation mechanisms of such materials would benefit from understanding the mechanisms of benzene reactions with AO.

The reactions of O(3P) and benzene have been studied by a variety of experimental methods. Relative reaction rates have been determined using static photolysis techniques.[1,2] Absolute reaction rate constants have been determined using pulsed radiolysis,[3] discharge flow,[4-6] modulation-phase shift,[7,8] and flash photolysis-NO_2 chemiluminescence[9] techniques. The entrance barrier of the O(3P) and benzene reaction has not been drawn explicitly, but is thought to be present from the gas phase determination of a 4 kcal/mol activation energy.[9] Crossed molecular beam experiments, carried out under single collision conditions with mean collision energies of 2.5 and 6.5 kcal/mol,[10] have shed some light on the reaction mechanism. Two distinct reaction channels were observed in this study:

$$O(3P) + C_6H_6 \rightarrow C_6H_5O\bullet + H\bullet \qquad (5.1)$$

$$O(3P) + C_6H_6 \rightarrow C_6H_5OH \qquad (5.2)$$

with the first channel (5.1) corresponding to hydrogen elimination and the other (5.2) to simple oxygen addition, presumably leading to phenol formation. The initial O(3P) electrophilic attack on benzene is believed to lead to a triplet biradical adduct whose lifetime is about $\leq$ 1 ns. This highly energetic reaction intermediate can then decay by a variety of channels: it can regenerate the reactants, eliminate a hydrogen atom with a small barrier of ~3-5 kcal/mol, or make a radiationless transition to a

singlet phenol. The branching ratio between the hydrogen elimination and intersystem crossing channels is energy dependent, with the intersystem crossing channel being favored by higher collision energy. Due to low collision energies used in this experiment hydrogen abstraction reactions leading to the formation of hydroxyl and phenyl radicals have not been observed.

If an aromatic ring is part of a polymer backbone, it has to be connected to the rest of the polymer chain by at least two bonds. An electrophilic O(3P) attack on π-electron density of benzene can occur at any of the six carbon atoms that make up the ring. According to the mechanism described above, a reactive collision of O(3P) with a carbon atom that is not bonded to the rest of the chain is not likely to disrupt the polymer backbone. A reactive collision of O(3P) with a carbon atom that is bonded to the rest of the chain, however, may result in a broken polymer backbone. Such reactions may be a very efficient degradation pathway (similar to the chain-breaking pathway described in detail in chapter 3 for degradation of aliphatic hydrocarbons) of materials containing aromatic rings in their backbone, given that activation energy for O(3P) and benzene reaction is very low, ~4 kcal/mol.[9] In this work we are particularly interested in determining the activation energies for O(3P) reactions with backbone fragments of various polymers that contain fragments of Ph-X-Ph type (where X can be any small group such as O, CO, $C(CH_3)_2$, etc.). Note that benzene can be viewed as Ph-H, and in the fragment mentioned above H is replaced by X-Ph. In this chapter we explore the reaction of benzene with O(3P) using various theoretical methods in order to determine their performance for such systems.

Computational Results

Formation of triplet intermediate: O(3P) + C_6H_6 → C_6H_6O (triplet). The key geometric parameters computed by *ab initio* and DFT methods of the transition state structure as well as the reactant (benzene) and product for the above reaction are presented in Table 5.1. The classical and vibrational adiabatic (zero-point corrected) reaction barriers and enthalpies obtained by various DFT and *ab initio* methods are presented in Table 5.2.

There is no experimental information that would suggest any information about the structure of the transition state or the triplet adduct product. Our calculations show that as the bond between O and C(1) (see Table 5.1) is formed, C(1) gradually becomes a center of a distorted tetrahedron, which implies an sp^3 hybridization for C(1). The C(1)-C(2) bond length increases almost reaching that of a single bond, while the C(2)-C(3) becomes essentially a double bond. The C(3)-C(4) bond is slightly longer than that in benzene. Thus, as the reaction proceeds, one π-electron of the ring forms a bond with the oxygen atom, while the other five π-electrons are delocalized on the remaining five carbon atoms. In both the transition state structure and the triplet adduct product, there exists a symmetry plane, which is perpendicular to the plane of the ring and dissects O, C(1), H(1), and C(4) atoms. While for different theoretical methods used there are differences in the computed structural parameters, all of the methods follow the trends described above.

Our best estimate for the activation energy of this reaction is that obtained with the use of CBS-QB3 method, 4.3 kcal/mol, which agrees well with the experimental result of –4 kcal/mol.[9] The values predicted with the use of HF and

MP2 methods are largely overestimated with respect to the experiment. DFT methods used predict small negative barriers.

TABLE 5.1: Structural parameters (ångstroms and degrees) for the reactant, product, and the transition state of C_6H_6 + O(3P) → C_6H_6O (triplet) reaction.

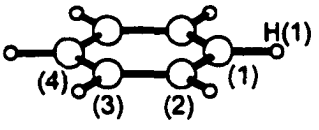

C_6H_6

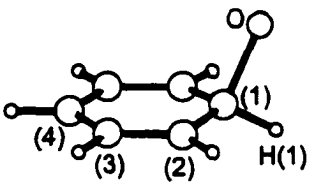

TS: $[C_6H_6O]^{\ddagger}$

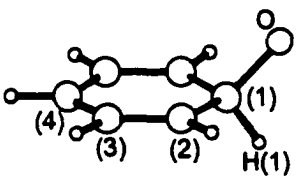

C_6H_6O

Theory	Species	r_{O-1}	r_{H1-1}	r_{1-2}	r_{2-3}	r_{3-4}	a_{O-1-H1}	$d_{O-1-2-3}$
HF/3-21G	C_6H_6	—	1.072	1.385	1.385	1.385	—	—
	TS	1.706	1.079	1.459	1.382	1.410	94.5	107.4
	C_6H_6O	1.467	1.094	1.500	1.373	1.416	101.3	129.2
HF/6-31G(d,p)	C_6H_6	—	1.076	1.386	1.386	1.386	—	—
	TS	1.797	1.074	1.449	1.386	1.410	95.6	100.0
	C_6H_6O	1.396	1.100	1.503	1.374	1.418	101.5	130.2
MP2(Full)/6-31G(d)	C_6H_6	—	1.087	1.395	1.395	1.395	—	—
	TS	1.858	1.084	1.416	1.362	1.388	94.6	94.1
	C_6H_6O	1.421	1.103	1.503	1.340	1.415	109.0	114.2
B3LYP/6-31+G (d,p)	C_6H_6	—	1.087	1.399	1.399	1.399	—	—
	TS	1.910	1.084	1.430	1.387	1.405	93.7	96.1
	C_6H_6O	1.393	1.126	1.508	1.369	1.419	99.4	129.8
B3LYP/6-311+G(2d,2p)	C_6H_6	—	1.082	1.392	1.392	1.392	—	—
	TS	1.902	1.079	1.425	1.380	1.399	93.7	96.1
	C_6H_6O	1.389	1.122	1.503	1.361	1.414	99.5	129.7
B3LYP/CBSB7	C_6H_6	—	1.084	1.394	1.394	1.394	—	—
	TS	1.883	1.082	1.429	1.382	1.401	94.8	95.2
	C_6H_6O	1.403	1.104	1.514	1.362	1.415	110.2	112.2
MB3LYP/6-31+G(d,p)	C_6H_6	—	1.087	1.399	1.399	1.399	—	—
	TS	1.909	1.084	1.431	1.387	1.405	93.6	96.4
	C_6H_6O	1.393	1.126	1.508	1.369	1.419	99.4	129.9

TABLE 5.2: Total energies (a. u.), enthalpies, and activation barriers (kcal/mol) for $C_2H_6 + O(3P) \rightarrow C_2H_6O$ (triplet) reaction.

Theory	E_{TS}	E_{C6H6}	E_O	E_{C6H6O}	ΔH	E_a
HF/3-21G	-303.78605	-229.41945	-74.39366	-303.79178	13.4	17.0
HF/3-21G (0 K)	-303.68024	-229.31061	-74.39366	-303.68549	**11.8**	**15.1**
HF/6-31G(d,p)	-305.47046	-230.71386	-74.78393	-305.49731	0.3	17.1
HF/6-31G(d,p) (0 K)	-305.36472	-230.60653	-74.78393	-305.39124	**-0.5**	**16.2**
MP2(Full)/6-31G(d)	-306.34574	-231.48719	-74.88329	-306.36599	2.8	15.5
MP2(Full)/6-31G(d) (0 K)	-306.24098	-231.38632	-74.88329	-306.26119	**5.3**	**18.0**
CBS-QB3 (0 K)	-306.77035	-231.78965	-74.98761	-306.79231	**-9.4**	**4.3**
B3LYP/6-31+G(d,p)	-307.33674	-232.26840	-75.06761	-307.36128	-15.9	-0.5
B3LYP/6-31+G(d,p) (0 K)	-307.23639	-232.16800	-75.06761	-307.26159	**-16.3**	**-0.5**
B3LYP/6-311+G(2d,2p)	-307.41095	-232.32067	-75.09006	-307.42473	-8.8	-0.1
B3LYP/6-311+G(2d,2p) (0 K)	-307.31078	-232.22036	-75.09006	-307.32420	**-8.6**	**-0.2**
MB3LYP/6-31+G(d,p)	-307.15018	-232.11206	-75.03772	-307.17505	-15.9	-0.3
MB3LYP/6-31+G(d,p) (0 K)	-307.04977	-232.01193	-75.03772	-307.07563	**-16.3**	**-0.1**

Effects of ortho and meta substitution on the activation energy of aromatic ring reaction with O(3P). Benzene reaction with O(3P) proceeds via electrophilic oxygen atom attack on the benzene ring π-electron density, the magnitude of which can be affected by electron-donating or electron-withdrawing substituents. Consequently, presence of such substituents may increase or decrease the activation energy for the reaction of aromatic ring with O(3P). Significant increase in the activation energy would be desirable, since that would imply higher LEO environment stability, and materials containing such substituents could be designed for LEO applications.

We chose a strong electron-donating substituent, NH_2, and strong electron-withdrawing substituent, CN. We studied the effects of two groups of the same kind (either NH_2 or CN) at both ortho and meta positions relative to the site of O(3P)

attack. The classical and vibrational adiabatic (zero-point corrected) reaction barriers obtained by HF and DFT methods for these reactions are presented in Table 5.3.

TABLE 5.3: Total energies (a. u.) and activation barriers (kcal/mol) for $C_2H_4X_2$ + O(3P) → $C_2H_4X_2O$ (triplet) reaction, where X = NH_2 or CN. The circles denote the site of O(3P) attack. HF stands for HF/3-21G method, and DFT denotes MB3LYP/6-31+G(d,p) method.

#	$C_2H_4X_2$	Theory	E_{TS}	E_{mol}	E_0	E_a
REF		HF	-303.78605	-229.41945	-74.39366	17.0
		HF (0 K)	-303.68024	-229.31061	-74.39366	**15.1**
		DFT	-307.15018	-232.11206	-75.03772	-0.3
		DFT (0 K)	-307.04977	-232.01193	-75.03772	**-0.1**
1		HF	-413.23674	-338.86951	-74.39366	16.6
		HF (0 K)	-413.09405	-338.72640	-74.39366	**16.3**
		DFT	X	-342.77714	-75.03772	X
		DFT (0 K)	X	-342.64361	-75.03772	X
2	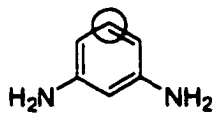	HF	-413.22733	-338.86951	-74.39366	22.5
		HF (0 K)	-413.08807	-338.72640	-74.39366	**20.1**
		DFT	-417.82105	-342.77714	-75.03772	-3.9
		DFT (0 K)	-417.68740	-342.64361	-75.03772	**-3.8**
3	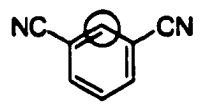	HF	-486.22657	-411.85199	-74.39366	12.0
		HF (0 K)	-486.12420	-411.74519	-74.39366	**9.2**
		DFT	-491.54075	-416.50548	-75.03772	1.5
		DFT (0 K)	-491.44326	-416.40808	-75.03772	**1.6**
4	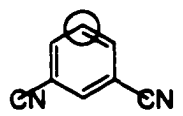	HF	-486.22111	-411.85199	-74.39366	15.4
		HF (0 K)	-486.11872	-411.74519	-74.39366	**12.6**
		DFT	-491.53887	-416.50548	-75.03772	2.7
		DFT (0 K)	-491.44181	-416.40808	-75.03772	**2.5**

It would seem that the electron-donating groups should decrease the activation barrier while the electron-withdrawing groups should increase the barrier. Indeed, the results obtained with the use of the DFT method follow these trends. The results obtained with the use of HF method, however, suggest the opposite. We draw conclusions based on the results obtained with the more accurate DFT method which, differently from HF, takes into account electron correlation. We find that the changes

in activation energy arising because of the substitution of the aromatic ring are rather small. For example, introduction of two CN groups at meta positions with respect to the reaction site raises the barrier by ~3 kcal/mol as compared to the case of benzene. The presence of two CN groups at ortho positions with respect to the reaction site, as expected, results in even smaller increase in activation energy, ~1.5 kcal/mol. Therefore, it is clear that while electron-donating or electron-withdrawing substituents do have an effect on the activation energy, the magnitude of it is too small in order to affect LEO AO erosion rates significantly.

Conclusions

We computed the activation energy of the aromatic ring reaction with O(3P) using several different theoretical methods. With the use of high level method, CBS-QB3, we obtained the activation energy of 4.3 kcal/mol, which agrees very well with experiment. Lower level methods fail to reproduce this number. Nevertheless, we have acquired the knowledge of how these methods perform for this system. Thus, we now have a way of calibrating the results for (larger) related systems.

While electron-donating or electron-withdrawing substituents do have an effect on the activation energy of this reaction, the magnitude of it is too small in order to affect LEO AO erosion rates significantly.

References

(1) Boocock, G.; Ćvetanovic, R. J. *Can. J. Chem.* **1961**, *39*, 2436.

(2) Grovenstein, Jr., E.; Mosher, A. J. *J. Am. Chem. Soc.* **1970**, *92*, 3810.

(3) Mani, L.; Sauer, M. C. *Adv. Chem. Ser.* **1968**, *82*, 142.

(4) Avramenko, L. I.; Kolesnikova, R. V.; Savinova, G. I. *Isv. Akad. Nauk. SSSR Ser. Khim 1965*. **1965**, *1*, 28.

(5) Bonanno, R. A.; Kim, P.; Lee, J.-H.; Timmons, R. B. *J. Chem. Phys.* **1972**, *57*, 1377.

(6) Furuyama, S.; Ebara, N. *Int. J. Chem. Kinet.* **1975**, *7*, 689.

(7) Atkinson, R.; Pitts, Jr., J. N. *J. Phys. Chem.* **1974**, *78*, 1780.

(8) Colussi, A. J.; Singleton, D. L.; Irwin, R. S.; Ćvetanovic, R. J. *J. Phys. Chem.* **1975**, *79*, 1900.

(9) Atkinson, R.; Pitts, Jr., J. N. *Chem. Phys. Lett.* **1979**, *63*, 485.

(10) Sibener, S. J.; Buss, R. J.; Casavecchia, P.; Hirooka, T.; Lee, Y. T. *J. Chem. Phys.* **1980**, *72*, 4341.

CHAPTER 6. AO Reactions with Molecules of Ph-X-Ph Type

Aromatic rings are present in the backbone of many polymers that are of interest to LEO spacecraft designers. In Table 6.1 we list examples of such materials. Almost all of these materials are made up entirely of fragments of Ph-X-Ph type, where Ph is a phenyl ring, and X is a small linkage group, such as O, CO, $C(CH_3)_2$, etc. (see Table 6.1). Polyimide and polybenzimidazole in addition to more complicated fragments also contain Ph-O-Ph and Ph-Ph (which does not have a linkage group) fragments, respectively.

As we pointed out in the previous chapter, a reactive collision of O(3P) with a carbon atom (in the aromatic ring) that is bonded to the rest of the chain may result in a broken polymer backbone. In this work we determine the activation energies for such O(3P) reactions with backbone fragments of various polymers that are of Ph-X-Ph type in order to determine whether such a mechanism is indeed plausible.

Computational Results

Formation of triplet intermediate: O(3P) + Ph-X-Ph → PhO-X-Ph (triplet). The classical and vibrational adiabatic (zero-point corrected) reaction barriers obtained by HF and DFT methods for all the Ph-X-Ph fragments of Table 6.1 are presented in Table 6.2.

TABLE 6.1: Polymeric materials with Ph-X-Ph fragments in their backbones. Circles denote the sites of reactions with O(3P) that we have studied in this work.

Name of Material	Structural Formula	Ph-X-Ph Fragments
Polyimide (Kapton®)	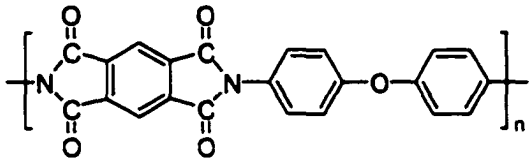	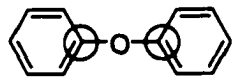
Polybenzimidazole (Celazole®)	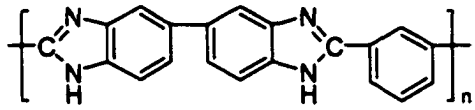	
Polyaramide (Kevlar®, Twaron®)	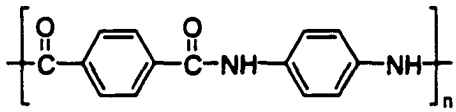	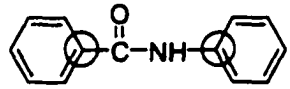
Polyetheretherketone (Victrex® PEEK, Hostatec®)	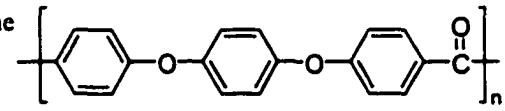	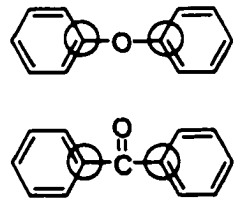
Polycarbonate (Makrolon®, Lexan®)	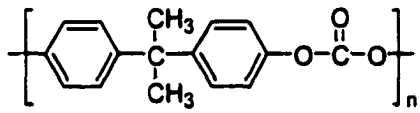	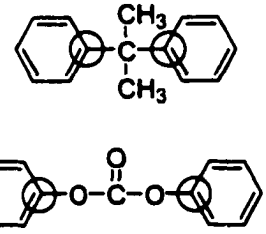
Polysulfone (Udel®, Ultrason®/S)	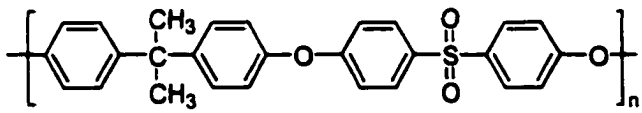	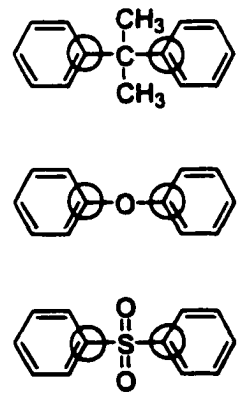

TABLE 6.2: Total energies (a. u.) and activation barriers (kcal/mol) for Ph-X-Ph + O(3P) → PhO-X-Ph (triplet) reaction, where X = O, CO, etc. The circles denote the site of O(3P) attack. HF stands for HF/3-21G method, and DFT denotes MB3LYP/6-31+G(d,p) method.

#	Ph-X-Ph	Theory	E_{TS}	E_{mol}	E_O	E_a
1	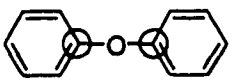	HF	-606.49066	-532.12649	-74.39366	18.5
		HF (0 K)	-606.29340	-531.92571	-74.39366	**16.3**
		DFT	-613.24560	-538.21202	-75.03772	2.6
		DFT (0 K)	-613.06095	-538.02713	-75.03772	**2.5**
2	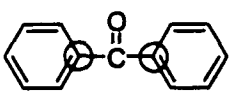	HF	-644.15524	-569.78756	-74.39366	16.3
		HF (0 K)	-643.95180	-569.57912	-74.39366	**13.2**
		DFT	-651.34603	-576.31107	-75.03772	1.7
		DFT (0 K)	-651.15529	-576.11984	-75.03772	**1.4**
3	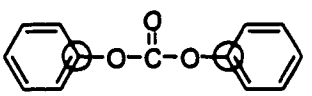	HF	-793.06249	-718.69362	-74.39366	15.6
		HF (0 K)	-792.84888	-718.47662	-74.39366	**13.4**
4A	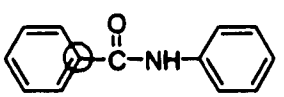	HF	-698.89868	-624.53419	-74.39366	18.3
		HF (0 K)	-698.67464	-624.30727	-74.39366	**16.5**
4B	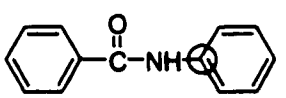	HF	-698.89310	-624.53419	-74.39366	21.8
		HF (0 K)	-698.67017	-624.30727	-74.39366	**19.3**
5	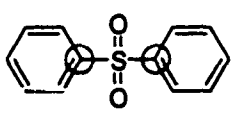	HF	-1076.56977	-1002.20629	-74.39366	18.9
		HF (0 K)	-1076.36500	-1001.99704	-74.39366	**16.1**
6	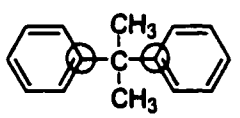	HF	-648.37525	-574.14033	-74.39366	99.6
		HF (0 K)	-648.09689	-573.85289	-74.39366	**93.9**
		DFT	-655.92048	-580.88507	-75.03772	1.4
		DFT (0 K)	-655.65514	X	-75.03772	X
6A		HF	-648.50992	-574.14033	-74.39366	15.1
		HF (0 K)	-648.22548	-573.85289	-74.39366	**13.2**
7		HF	-532.05521	-457.68867	-74.39366	17.0
		HF (0 K)	-531.86251	-457.49236	-74.39366	**14.7**

We observed previously (Chapter 5) that the calculated barriers for O(3P) reaction with benzene obtained with the use of HF and DFT methods differed by ~15 kcal/mol. Similar trends exist in the case of the fragments of Ph-X-Ph type. The barrier for the Ph-O-Ph (#1 from Table 6.2) reaction with O(3P) is 16.3 kcal/mol and 2.5 kcal/mol as obtained with the use of HF and DFT methods, respectively. The barrier for the Ph-CO-Ph (#2 from Table 6.2) reaction with O(3P) is 13.2 kcal/mol and 1.4 kcal/mol as obtained with the use of HF and DFT methods, respectively. The barrier for the Ph-$C(CH_3)_2$-Ph (#6 from Table 6.2) reaction with O(3P) is 93.9 kcal/mol and 79.2 kcal/mol as obtained with the use of HF and DFT methods, respectively. The rest of the fragments were calculated with the use of the less expensive HF method only. However, the relative consistency of the two methods demonstrated for the above three examples gives us enough confidence in the rest of the results. In addition, based on our experience with benzene, we believe that the HF method overestimates the energy value of the reaction barrier, while the DFT method underestimates the energy value of the reaction barrier.

The HF calculated barriers for all fragments (except #6, Ph-$C(CH_3)_2$-Ph, which is discussed later in this chapter) in Table 6.2 range between ~13 and ~19 kcal/mol. Based on our previous experience with a more accurate theoretical method, CBS-QB3, applied to the case of benzene, we estimate that the more accurate values would have to be ~5 to ~8 kcal/mol. The implication of this result is that all of the polymers listed in Table 6.1 as well as many others that have similar structures are highly susceptible to AO attack in LEO, where oxygen atoms possess translational energy on the order of 100 kcal/mol.

Reactions of Ph-O-Ph fragment with O(3P). We examine this particular case in more detail here. We look not only into the formation of triplet adduct product of O(3P) attack on a carbon atom (in the aromatic ring) that is bonded to the rest of the polymer chain, but also determine the barrier for the subsequent "chain breaking" (similar to hydrogen elimination in the case of benzene) reaction.

The key geometric parameters computed by HF and DFT methods for all the structures leading to the "chain breaking" by O(3P) in Ph-O-Ph fragment are presented in Table 6.3. The absolute energies for all the structures of Table 6.3 are listed in Table 6.4. An energy diagram of the "chain breaking" process is depicted in Figure 6.1.

Thus, the "chain breaking" by O(3P) in Ph-O-Ph may proceed as follows. Ph-O-Ph molecule (Table 6.3, top left) is attacked by a triplet oxygen atom. The reaction proceeds via the transition state, TS1 (Table 6.3, top right), which lies energetically higher than the reactants by 2.5 kcal/mol and 16.3 kcal/mol as computed with DFT and HF methods, respectively (see Figure 6.1). As pointed out above, this barrier can be better estimated at ~5 to ~8 kcal/mol. Consequently, a triplet intermediate adduct is formed (Table 6.3, bottom left). This species can subsequently undergo a C1-O_B bond scission via the transition state, TS2 (Table 6.3, bottom middle), with a low ~4 kcal/mol barrier as computed with both HF and DFT methods (see Figure 6.1). Finally, two Ph-O radicals (Table 6.3, bottom right) are formed.

TABLE 6.3: Structural parameters (ångstroms and degrees) for all the structures leading to the "chain breaking" in Ph-O-Ph fragment by O(3P).

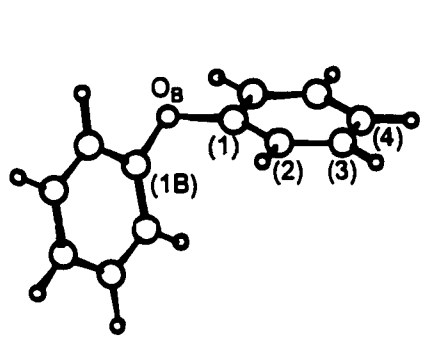

C_6H_5-O-C_6H_5

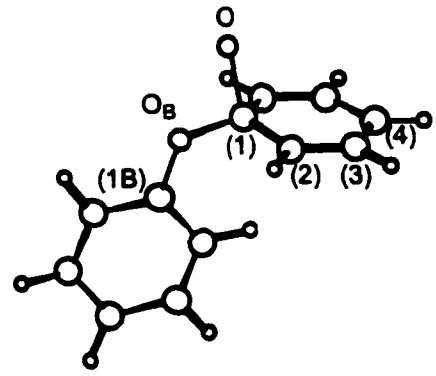

TS1: [C_6H_5-O-C_6H_5O]‡

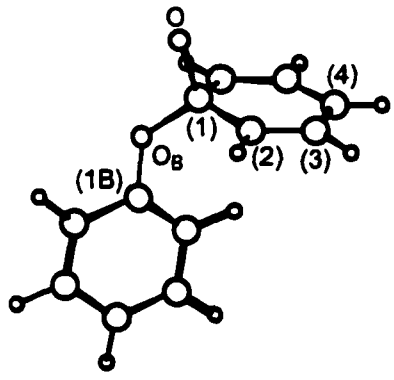

C_6H_5-O-C_6H_5O

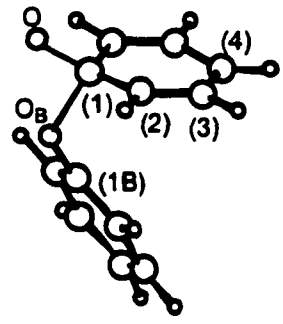

TS2: [C_6H_5O–C_6H_5O]‡

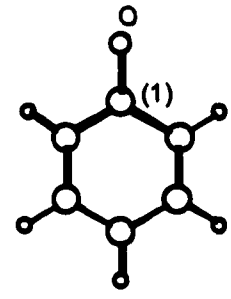

C_6H_5O

Theory	Species	r_{O-1}	r_{1-OB}	r_{OB-1B}	a_{O-1-OB}	$d_{2-1-OB-1B}$	$d_{O-1-2-3}$
HF/3-21G	C_6H_5-O-C_6H_5	—	1.390	1.390	—	40.7	—
	TS1	1.700	1.410	1.390	94.5	71.8	101.1
	C_6H_5-O-C_6H_5O	1.438	1.425	1.382	104.9	65.7	106.6
	TS2	1.408	1.636	1.383	94.6	80.2	147.0
	C_6H_5O	1.308	—	1.308	—	—	—
MB3LYP/6-31+G(d,p)	C_6H_5-O-C_6H_5	—	1.384	1.384	—	39.5	—
	TS1	1.928	1.386	1.384	97.6	87.4	90.5
	C_6H_5-O-C_6H_5O	1.357	1.440	1.376	107.7	60.3	105.5
	TS2	1.313	1.684	1.348	103.3	73.2	137.6
	C_6H_5O	1.261	—	1.261	—	—	—

TABLE 6.4: Total energies (a. u.) for all the structures leading to the "chain breaking" in Ph-O-Ph fragment by O(3P).

Theory	C_6H_5-O-C_6H_5	TS1	C_6H_5-O-C_6H_5O	TS2	C_6H_5O
HF/3-21G	-532.12649	-606.49066	-606.50062	-606.49171	-303.27755
HF/3-21G (0 K)	-531.92571	-606.29340	-606.30092	-606.29523	-303.18048
MB3LYP/6-31+G(d,p)	-538.21202	-613.24560	-613.27746	-613.26824	-306.66669
MB3LYP/6-31+G(d,p) (0K)	-538.02713	-613.06095	-613.09264	-613.08558	-306.57530

Figure 6.1. Energy diagram of the Ph-O-Ph "chain breaking" by O(3P) process. The energy values are in units of kcal/mol, and have been calculated with the use of HF/3-21G (italics) and MB3LYP/6-31+G(d,p) (boldface) methods.

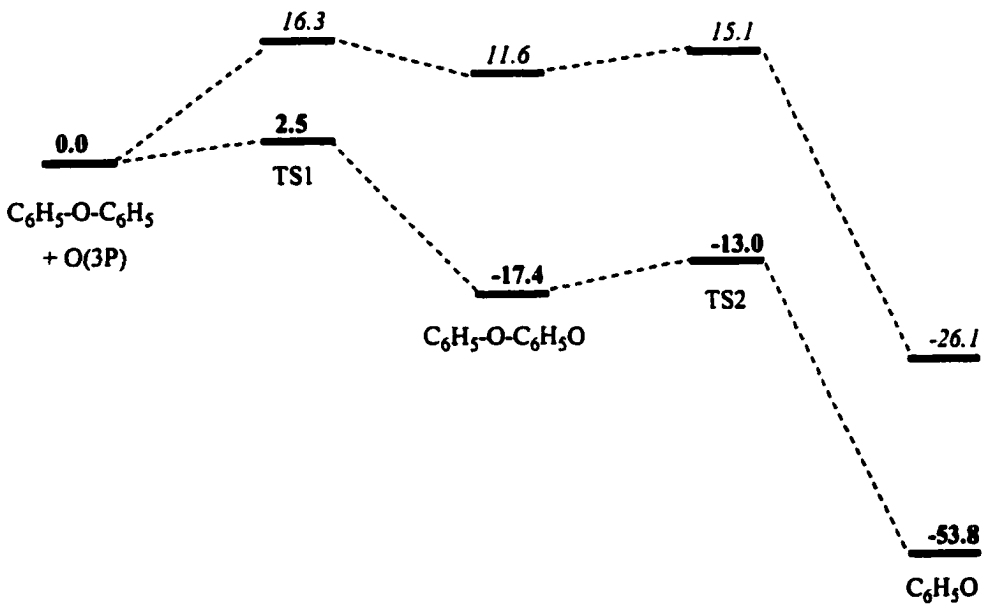

Reasons for high activation energy of the reaction: O(3P) + Ph-C$(CH_3)_2$-Ph → PhO- C$(CH_3)_2$-Ph (triplet). The very high barrier for the Ph-C$(CH_3)_2$-Ph (#6 from Table 6.2) reaction with O(3P) (93.9 kcal/mol as obtained with the use of the HF method) deserves particular attention. Table 6.4 shows the structure of Ph-C$(CH_3)_2$-Ph on the left, and two possible transition state structures leading to the formation of the triplet adduct product on the right. There exist two transition state structures because oxygen atom can attack the phenyl ring from two different sides with respect to the orientation of the methyl groups. The high energy barrier is observed for the pathway where oxygen atom attacks the same side that the methyl groups are facing. Therefore, the repulsion between oxygen atom and the methyl groups must be the cause of such a high barrier. If oxygen atom attacks from another side, however, the value for the energy barrier is in the same range as for all other fragments (#6A, Table 6.2). The above conclusion is supported by examination of geometrical parameters such as the forming O-C bond length in the transition state structure (see Table 6.5). This bond is much longer than the corresponding bond in the lower energy transition state of the same molecule.

The barrier for the Ph-C$(CH_3)_2$-Ph (#6 from Table 6.2) reaction with O(3P) obtained with the use of the DFT method is ~1 kcal/mol as opposed to >90 kcal/mol as computed with the HF method. We will therefore attempt to investigate this case in more detail in future.

TABLE 6.5: Structural parameters (ångstroms and degrees) of Ph-C$(CH_3)_2$-Ph and two possible transition state structures leading to the formation of the triplet adduct product.

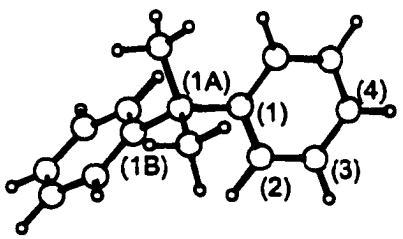

C_6H_5-C$(CH_3)_2$-C_6H_5

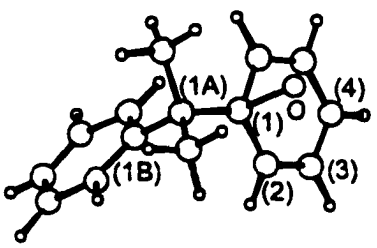

TS(A): [C_6H_5-O-C_6H_5O]‡

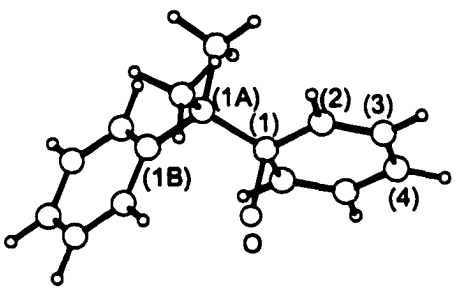

TS(B): [C_6H_5-O-C_6H_5O]‡

Theory	Species	$r_{O\text{-}1}$	$r_{1\text{-}1A}$	$a_{O\text{-}1\text{-}1A}$	$d_{2\text{-}1\text{-}1A\text{-}1B}$	$d_{O\text{-}1\text{-}2\text{-}3}$
HF/3-21G	C_6H_5-C$(CH_3)_2$-C_6H_5	—	1.538	—	50.6	—
	TS(A)	1.928	1.546	101.3	64.8	85.6
	TS(B)	1.755	1.553	104.6	44.7	96.4
MB3LYP/6-31+G(d,p)	C_6H_5-C$(CH_3)_2$-C_6H_5	—	1.543	—	50.3	—
	TS(A)	1.926	1.556	102.9	67.7	88.8
	TS(B)	X	X	X	X	X

Conclusions

We calculated the activation energies for AO attack of the aromatic ring at its junction to the rest of the polymer chain, estimating a magnitude of only ~5-8 kcal/mol. Since aromatic rings themselves are such stable entities it may perhaps seem surprising that these polymers degrade at rates comparable to those of materials made up of aliphatic hydrocarbons. However, the rapid degradation is, in fact, consistent with the very low activation energy we determined. We found that the electron donor/acceptor properties of the linkage groups connecting the aromatic rings leaves the activation energies largely unaffected. However, the steric effects of the linkage groups when they are bulky can increase the activation energy greatly. This fact might be suggestive of a general method for designing materials of this type that are less susceptible to erosion. It is important to realize that even though a total protection of any given material may not be possible, any material design, which slows the rate of degradation significantly, may be of great value.

CHAPTER 7. A Possible Correlation of Structure and Erosion Rate

The ultimate goal of our research is the ability to correlate materials LEO erosion rates to their structure. This is not a straightforward task due to complexity of materials degradation mechanisms by AO and lack of reliable experimental data from space experiments. The latter will soon change since space experiments for determining accurate erosion rates for many materials under the same conditions are anticipated in near future.

Nevertheless, based on the experimental data that are available now, and the degradation mechanisms that we studied using quantum chemistry methods, we believe that at this point we are able to predict LEO erosion rates from the materials structure for a certain class of polymers, viz., the materials listed in Table 7.1. The backbone of these polymers consists almost entirely of aromatic rings linked together by small linkage groups, and none of them contain aliphatic hydrocarbon fragments.

Based on the results of chapters 5-6, we believe that the rate-determining step in the degradation process of these polymers is the chain breaking reactions at "weak spots" (WS) of the polymer backbone caused by a single O(3P) attack. We give the name of WS to the backbone sites where the reaction with O(3P) occurs with a very low activation energy, ~5 to 8 kcal/mol, and can subsequently lead to a broken chain. Such sites are denoted by circles in Table 7.1. We arbitrarily assign a count of ½ of WS (denoted by squares in Table 7.1) to the sites which we believe to be half as effective in the degradation process. For example, for the Ph-$C(CH_3)_2$-Ph fragment, for which the reaction with O(3P) occurs with low activation energy only for oxygen

atom attack from one phenyl ring side, and not from the other (see Chapter 6), we assign two ½ of WS instead of two WS. The reasoning for the polyimide is that the reaction has to occur twice in order for the chain to be broken.

TABLE 7.1: Count of "Weak Spots" in the materials.
WS – "weak spot"
k – number of WS present in a polymer repeat unit
Circle – counted as WS
Square – counted as ½ WS

Name of Material	Structural Formula	k
Polyimide (Kapton®)	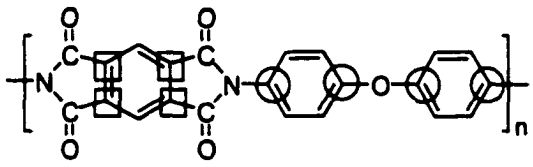	6
Polyaramide (Kevlar®, Twaron®)	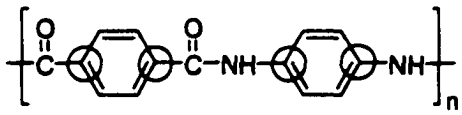	4
Polyetheretherketone (Victrex® PEEK, Hostatec®)	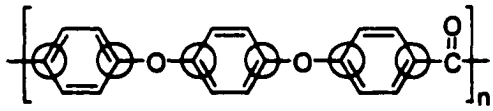	6
Polysulfone (Udel®, Ultrason®/S)	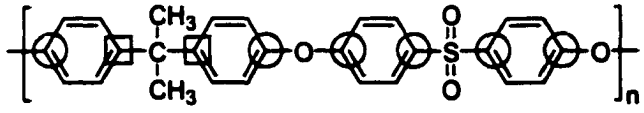	7

Since the activation energies for the reactions at "weak spots" are very low relative to translational energy possessed by AO in LEO environment, to a good approximation they can be considered the same. Therefore the degradation rates of materials should be proportional only to the density of "weak spots", D (mol/cm^3):

$$D = kd/M,$$

where k is the number of WS in polymer repeat unit, d is the density of the material in mol/cm^3, and M is the molar mass of polymer repeat unit in g/mol. All of these parameters and also the LEO erosion rates are listed in Table 7.2 for all the materials from Table 7.1.

TABLE 7.2: Density of "Weak Spots", D = kd/M, and LEO Erosion of the materials.

Name of Material	Formula	M, g/mol	d, g/cm^3	d/M, $\times10^{-3}$ mol/cm^3	k	D, mol/cm^3	LEO Erosion,[a] $\times10^{-24}$ cm^3/O-atom
Polysulfone (Udel®, Ultrason®/S)	$C_{27}H_{22}O_4S$	442.53	1.24	2.80	7	**0.020**	**2.3**
Polyimide (Kapton®)	$C_{22}H_{10}O_5N_2$	382.33	1.43	3.74	6	**0.022**	**3.0**
Polyaramide (Kevlar®, Twaron®)	$C_{14}H_{10}O_2N_2$	238.25	1.45	6.09	4	**0.024**	**4.0**
Polyetheretherketone (Victrex® PEEK, Hostatec®)	$C_{19}H_{12}H_3$	288.30	1.30	4.51	6	**0.027**	**4.7** **2.3**

[a]The LEO erosion data is from ref. 1.

Subsequently, Figure 7.1 presents a plot of LEO erosion vs. density of WS for materials. The linear dependency of LEO erosion vs. density of WS is consistent with the mechanism described above. While the LEO erosion results for some of the

materials have been reproduced (polyimide and polysulfone) during at least two different experiments, for one of the materials, PEEK, however, there exist only two experimental results, and they are very different. One of these results does happen to fall on the line in Figure 7.1. This might be an indication that the other experiment went wrong, or that our proposed correlation does not hold. Future experiments hopefully will resolve the issue.

Figure 7.1. Plot of LEO Erosion vs Density of "Weak Spots" for materials.

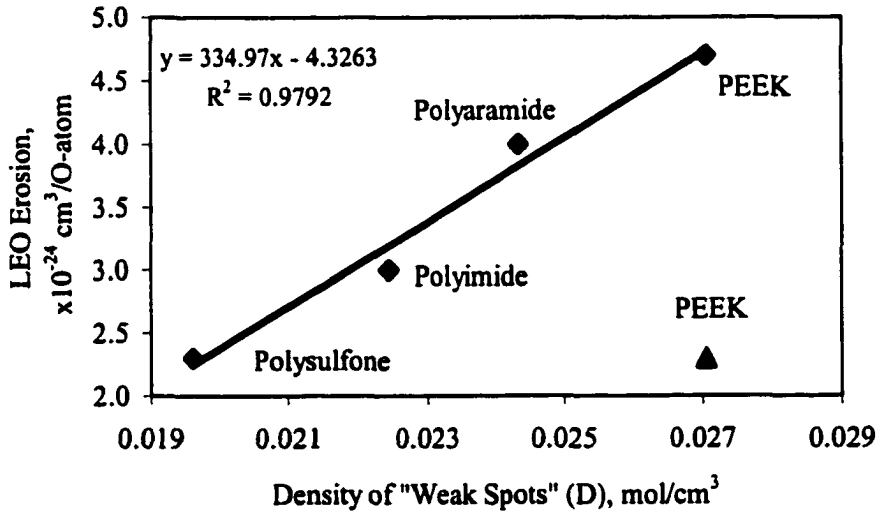

Note that the obtained correlation equation (Figure 7.1) might easily be applied for prediction of the erosion rates of other materials that fall in the category of materials listed in Table 7.1. For example, polycarbonate (Makrolon®, Lexan®) falls into this category. It is absent from our correlation plot due to absence of LEO erosion data. However, it will be interesting to see, whether the LEO erosion rate

predicted for this material using our correlation equation will agree with the results obtained from future space experiments. We considered including polybenzimidazole (Celazole®) in our correlation chart, since the polymer repeat unit of this material also possesses sites that agree with our definition of the "weak spots", however, the additional structural differences precluded us from doing so.

References

(1) Banks, B. A. "The Use of Fluoropolymers in Space Applications" In *Modern Fluoropolymers*; John Wiley & Sons: New York, 1997 and references therein.

CHAPTER 8. Concluding Remarks

In this work we have used quantum mechanics to study the important problem of polymers degradation in low Earth orbit due to chemical reactions with atomic oxygen.

We studied a class of compounds called aliphatic hydrocarbons. It has been previously assumed that the important degradation mechanism was hydrogen abstraction. However, we considered the possibility that a chain breaking mechanism might be an important contributor to the degradation. We found that the activation energy for the chain breaking mechanism was ~40-45 kcal/mol, significantly less than the translational energy available to AO in LEO.

Fluorocarbon material Teflon® has a structure similar to that of aliphatic hydrocarbons, except that fluorine is substituted for hydrogen. Previously it has been unclear whether AO alone (i. e., in absence of UV) could contribute to its erosion. We found the activation energy for chain breaking in Teflon® to be approximately ~70-80 kcal/mol. This is significantly lower than the ~100 kcal/mol translational energy available to AO in LEO and therefore, this mechanism is a definite possible contributor to the degradation. But this is also significantly higher than the ~40-45 kcal/mol activation energy for aliphatic hydrocarbons which implies that the rate of degradation for Teflon® would be much lower than for those materials, which is consistent with the experimental results.

Polymers containing aromatic rings in their backbone are highly susceptible to AO erosion. We calculated the activation energies for AO attack of the aromatic ring at its junction to the rest of the polymer chain, finding a magnitude of only ~5-8

kcal/mol. Because aromatic rings themselves are such stable entities it may perhaps seem surprising that these polymers degrade at quite a high rate. However, the rapid degradation is, in fact, consistent with the very low activation energy we determined. We found that the electron donor/acceptor properties of either ortho/meta substituents or the linkage groups connecting the aromatic rings leaves the activation energies largely unaffected. However, the steric effects of the linkage groups when they are bulky may increase the activation energy greatly. This fact might be suggestive of a general method for designing materials of this type that are less susceptible to AO erosion. It is important to realize that even though a total protection of any given material may not be possible, any material design, which slows the rate of degradation significantly, may be of great value.

The presence of so many "weak spots" associated with polymers that possess "aromatic backbones" caused us to speculate that they, in fact, may be the rate determining factor in their degradation. Therefore, we chose example polymers having a backbone consisting almost entirely of aromatic rings hooked together by small linkage groups with a view to correlate the density of their "weak spots" and their LEO erosion rates. Interestingly, at least for the four polymers, for which we happen to have measured LEO erosion data, a linear correlation was found. Whether or not this correlation is more general awaits further testing.

We mention that we have thus far looked at two types of materials, which we have called aliphatic chains and "aromatic backbones". In fact, we have chosen these two types of materials because they have a certain simplicity of structure. The study of relevant reaction mechanisms is simplified somewhat by these choices of materials

for study. In the case of "aromatic backbones" in so far as the linear correlation between the density of "weak spots" and the erosion rates is correct, that is consistent with the importance of the "aromatic backbone" chain-breaking mechanism. We anticipate that in more complicated cases involving polymers which have both aromatic rings and fragments of aliphatic hydrocarbons the simple linear correlation referred to above might break down. This is because of additional important mechanisms, which would prevent the aromatic chain-breaking mechanism from being the only rate-determining factor. However, in such cases, even though the linear correlation breaks down, we would still expect the aromatic chain breaking mechanism to be relatively important because of its very low activation energy.

Finally, we point out we have established a computationally effective scheme to study these reaction mechanisms. We have struck a balance between quantity and quality of calculations, which has allowed us to advance our problem. This balance will be of value to future workers investigating related systems.

BIBLIOGRAPHY

Chapter 1

(1) Banks, B. A.; de Groh, K. K.; Rutledge, S.; DiFilippo, F. J. NASA TM-107209, **1996**.

(2) Leger, L. J. NASA TM-58246, **1982**.

(3) Leger, L. J.; Visentine, J. T. *Aerospace America* **1986**, *24*, 32.

(4) Hunton, D. E. "Shuttle Glow." *Sci. Am.* **1989**, *261*, 92.

(5) Murr, L. E.; Kinard, W. H. "Effects of Low Earth Orbit." *Amer. Sci.* **1993**, *81*, 152.

(6) Reddy, M. R. *J. Mat. Sci.* **1995**, *30*, 281.

(7) Banks, B. A. "The Use of Fluoropolymers in Space Applications" In *Modern Fluoropolymers*; John Wiley & Sons: New York, **1997** and references therein.

(8) Gregory, J. NASA CP-3257.

(9) Dooling, D.; Finckenor, M. M. NASA TP-209260, **1999**.

(10) Leger, L. J. AIAA Paper 83-0073, **1983**.

(11) Peters, P. N.; Linton, R. C.; Miller, E. R. *Geophys. Res. Lett.* **1983**, *10*, 569.

(12) Leger, L. J., Spiker, I. K.; Kuminecz, T. J.; Ballentine, T. J.; Visentine, J. T. AIAA Paper 83-2631, **1983**.

(13) Park, J. J.; Gull, T. R.; Herzing, H.; Toft, A. R. AIAA Paper 83-2634, **1983**.

(14) Slemp, W. S. AIAA Paper 83-2633, **1983**.

(15) Visentine, J. T. NASA TM-100459, **1988**.

(16) Tennyson, R. C.; Morision, W. D.; Klemberg, J. E.; Martinu, L.; Wertheimer, M. R.; Zimick, D. G. AIAA Paper 92-2152, **1992**.

(17) Dunnet, A.; Kirkendal, T. D. in *Proceedings of the European Space Power Conference*; ESA-SP **1991**, *320*, 701.

(18) Levine, A. S. NASA CP-3134, **1992**.

(19) Levine, A. S. NASA CP-3194, **1993**.

(20) Schwam, D. *Space* **1993**, *9*, 14.

(21) Srinivasan, V.; Banks, B. A., Eds. *Materials Degradation in Low Earth Orbit*, Warrendale, Pa.: The Minerals, Metals and Materials Society, **1990**.

(22) Minton, T. K.; Nelson, C. M.; Brinza, D. E.; Liang, R. H. JPL, *Publication 91-34*, **1991**.

(23) Banks, B. A.; Rutledge, S. K.; Paulsen, P. E.; Steuber, T. J. NASA TM-101971, **1989**.

(24) Rutledge, S. K.; Banks, B. A.; DiFilippo, F.; Brady, J. A.; Dever, T.; Hotes, D. NASA TM-100122, **1986**.

(25) Garton, D. J.; Minton, T. K.; Alagia, M.; Balucani, N.; Casavecchia, P.; Volpi, G. G. *Discuss. Faraday Soc.* **1997**, *108*, 387.

(26) Kleiman, J. I.; Gudimenko, Y. I.; Iskanderova, Z. A.; Tennyson, R. C.; Morison, W. D.; McIntyre, M. S.; Davidson, R. *Surface and Interface Analysis* **1995**, *23*, 335.

(27) Iskanderova, Z. A.; Kleiman, J. I.; Gudimenko, Y. I.; Tennyson, R. C. *J. Spacecraft Rockets*, **1995**, *32*, 878.

Chapter 2

(1) Frisch, M. J.; Trucks, G. W.; Schlegel, H. B.; Scuseria, G. E.; Robb, M. A.; Cheeseman, J. R.; Zakrzewski, V. G.; Montgomery, J. A., Jr.; Stratmann, R. E.; Burant, J. C.; Dapprich, S.; Millam, J. M.; Daniels, A. D.; Kudin, K. N.; Strain, M. C.; Farkas, O.; Tomasi, J.; Barone, V.; Cossi, M.; Cammi, R.; Mennucci, B.; Pomelli, C.; Adamo, C.; Clifford, S.; Ochterski, J.; Petersson, G. A.; Ayala, P. Y.; Cui, Q.; Morokuma, K.; Malick, D. K.; Rabuck, A. D.; Raghavachari, K.; Foresman, J. B.; Cioslowski, J.; Ortiz, J. V.; Stefanov, B. B.; Liu, G.; Liashenko, A.; Piskorz, P.; Komaromi, I.; Gomperts, R.; Martin, R. L.; Fox, D. J.; Keith, T.; Al-Laham, M. A.; Peng, C. Y.; Nanayakkara, A.; Gonzalez, C.; Challacombe, M.; Gill, P. M. W.; Johnson, B.; Chen, W.; Wong, M. W.; Andres, J. L.; Gonzalez, C.; Head-Gordon, M.; Replogle, E. S.; Pople, J. A. *Gaussian 98*, Revision A.6; Gaussian, Inc.: Pittsburgh PA, **1998**.

(2) MULLIKEN is IBM proprietary software.

(3) Foresman, J. B.; Frisch, A. *Exploring Chemistry with Electronic Structure Methods*, 2nd ed.; Gaussian, Inc.: Pittsburgh, **1996**.

(4) Roothan, C. C. J.; *Rev. Mod. Phys.* **1951**, *23*, 69.

(5) Pople, J. A.; Nesbet, R. K. *J. Chem. Phys.* **1959**, *22*, 571.

(6) McWeeny, R.; Dierksen, G. *J. Chem. Phys.* **1968**, *49*, 4852.

(7) Möller, C.; Plesset, M. S. *Phys. Rev.* **1934**, *46*, 618.

(8) Saebo, S.; Almlof, J. *Chem. Phys. Lett.* **1989**, *154*, 83.

(9) Pople, J. A.; Binkley, J. S.; Seeger, R. *Int. J. Quant.Chem. Symp.* **1976**, *10*, 1.

(10) Becke, A. D. *J. Chem. Phys.* **1993**, *98*, 5648.

(11) Lee, C.; Yang, W.; Parr, R. G. *Phys. Rev. B* **1988**, *37*, 785.

(12) Perdew, J. P. *Phys. Rev. B* **1986**, *33*, 8822.

(13) Perdew, J. P. *Phys. Rev. B* **1987**, *34*, 7046.

(14) Perdew, J. P.; Wang, Y. *Phys. Rev. B* **1992**, *45*, 13244.

(15) P. J. Stephens, F. J. Devlin, C. F. Chabalowski,M. J. Frisch, *J. Phys. Chem.* **1994**, *98*, 11623. MB3LYP is very similar to B3LYP defined in this paper, except it uses the local correlation functional of Perdew and Wang (J. P. Perdew, Y. Wang, *Phys Rev. B* **1992**, *45*, 1324) instead of the Vosko, Wilk and Nusair functional.

(16) Montgomery, Jr., J. A.; Frisch, M. J.; Ochterski, J. W.; Petersson, G. A. *J. Chem. Phys.* **1999**, *110*, 2822.

(17) Pople, J. A.; Head-Gordon, M.; Fox, D. J.; Raghavachari, K.; Curtiss, L. A. *J. Chem. Phys.* **1989**, *90*, 5622.

(18) Curtiss, L. A.; Jones, C.; Trucks, G. W.; Raghavachari, K.; Pople, J. A. *J. Chem. Phys.* **1990**, *93*, 2537.

(19) Curtiss, L. A.; Raghavachari, K.; Trucks, G. W.; Pople, J. A. *J. Chem. Phys.* **1991**, *94*, 7221.

(20) Curtiss, L. A.; Raghavachari, K.; Pople, J. A. *J. Chem. Phys.* **1993**, *98*, 1293.

(21) Scott A. P.; Radom L. *J. Phys. Chem.* **1996**, *100*, 16502.

Chapter 3

(1) Banks, B. A. "The Use of Fluoropolymers in Space Applications." In *Modern Fluoropolymers*; John Wiley & Sons: New York, **1997**.

(2) Koontz, S. L.; Albyn, K. A.; Leger, L. J. "Atomic Oxygen Testing with Thermal Atom Systems: A Critical Evaluation." *J. Spacecraft Rockets* **1991**, *28*, 315.

(3) Tennyson, R. C. "Atomic Oxygen Effects on Polymer-Based Materials." *Can. J. Phys.* **1991**, *69*, 1190.

(4) Chambers, A. R.; Harris, I. L.; Roberts, G. T. "Reactions of Spacecraft Materials with Fast Atomic Oxygen." *Materials Letters* **1996**, *26*, 121.

(5) Garton, D. J.; Minton, T. K.; Alagia, M.; Balucani, N.; Casavecchia, P.; Volpi, G. G. "Reactive Scattering of Ground-State and Electronically-Excited Oxygen Atoms on a Liquid Hydrocarbon Surface." *Discuss. Faraday Soc.* **1997**, *108*, 387.

(6) Cazaubon, B.; Paillous A.; Siffre, J. "Mass Spectrometric Analysis of Reaction Products of Fast Oxygen Atoms-Materials Interactions." *J. Spacecraft Rockets* **1998**, *35*, 797.

(7) Jursic, B. S. *J. Mol. Struct. (THEOCHEM)* **1998**, *427*, 137.

(8) Andresen, P.; Luntz, A. C. *J. Chem. Phys.* **1980**, *72*, 5842.

(9) Gonzalez, C.; MacDouall, J. J. M.; Schlegel, H. B. *J. Phys. Chem.* **1990**, *94*, 7467 and references therein.

Chapter 4

(1) Banks, B. A. "The Use of Fluoropolymers in Space Applications." In *Modern Fluoropolymers*; John Wiley & Sons: New York, **1997**.

(2) Rutledge, S. K.; Banks, B. A.; Kitral, M. "A Comparison of Space and Ground Based Facility Environmental Effects for FEP Teflon." NASA TM-207918/REV1, **1998**.

(3) Koontz, S. L.; Leger, L. J.; Albyn, K. A.; Cross, J. "Ultraviolet Radiation/Atomic Oxygen Synergism in Materials Reactivity." *J. Spacecraft and Rockets* **1990**, *27*, 346.

(4) Kim, S. S.; Liang, R. H. *Polym. Prepr.* **1990**, *31*, 389.

(5) Rasoul, F. A.; Hill, D. J. T.; George, G. A.; O'Donnell J. H. "A Study of a Simulated Low Earth Environment on the Degradation of FEP Polymer." *Polymers for Advanced Technologies* **1998**, *9*, 24.

(6) Rousslang, K.; Crutcher, Pippin, H. G. Proceedings of the First LDEF Post-retrieval Symposium, NASA CP-3134(2), 847, **1992**.

(7) Chambers, A. R.; Harris, I. L.; Roberts, G. T. "Reactions of Spacecraft Materials with Fast Atomic Oxygen." *Materials Letters* **1996**, *26*, 121.

(8) Vered, R.; Matlis, S.; Nahor, G.; Lempert, G. D.; Grossman, E.; Marom, G.; Lifshitz, Y. *Surface and Interface Analysis* **1994**, *22*, 532.

(9) Tennyson, R. C. "Atomic Oxygen Effects on Polymer-Based Materials." *Can. J. Phys.* **1991**, *69*, 1190.

(10) Reddy, M. R. "Review Effect of Low Earth Orbit Atomic Oxygen on Spacecraft Materials" *J. Mat. Sci.* **1995**, *30*, 281.

Chapter 5

(1) Boocock, G.; Ćvetanovic, R. J. *Can. J. Chem.* **1961**, *39*, 2436.

(2) Grovenstein, Jr., E.; Mosher, A. J. *J. Am. Chem. Soc.* **1970**, *92*, 3810.

(3) Mani, L.; Sauer, M. C. *Adv. Chem. Ser.* **1968**, *82*, 142.

(4) Avramenko, L. I.; Kolesnikova, R. V.; Savinova, G. I. *Isv. Akad. Nauk. SSSR Ser. Khim 1965.* **1965**, *1*, 28.

(5) Bonanno, R. A.; Kim, P.; Lee, J.-H.; Timmons, R. B. *J. Chem. Phys.* **1972**, *57*, 1377.

(6) Furuyama, S.; Ebara, N. *Int. J. Chem. Kinet.* **1975**, *7*, 689.

(7) Atkinson, R.; Pitts, Jr., J. N. *J. Phys. Chem.* **1974**, *78*, 1780.

(8) Colussi, A. J.; Singleton, D. L.; Irwin, R. S.; Ćvetanovic, R. J. *J. Phys. Chem.* **1975**, *79*, 1900.

(9) Atkinson, R.; Pitts, Jr., J. N. *Chem. Phys. Lett.* **1979**, *63*, 485.

(10) Sibener, S. J.; Buss, R. J.; Casavecchia, P.; Hirooka, T.; Lee, Y. T. *J. Chem. Phys.* **1980**, *72*, 4341.

Chapter 7

(1) Banks, B. A. "The Use of Fluoropolymers in Space Applications" In *Modern Fluoropolymers*; John Wiley & Sons: New York, 1997 and references therein.